JBC Papers in Press. Published on December 12, 2018 as Manuscript RA118.004110
The latest version is at http://www.jbc.org/cgi/doi/10.1074/jbc.RA118.004110

Cytochrome c auto-catalyzed carbonylation in the presence of hydrogen peroxide and cardiolipins

Uladzimir Barayeu[1,2,3,#] , Mike Lange[1,2,#], Lucía Méndez [1,2,4], Jürgen Arnhold[3], Oleg I. Shadyro[5], Maria Fedorova[1,2,*], and Jörg Flemmig[3,*]

[1]Institute of Bioanalytical Chemistry, Faculty of Chemistry and Mineralogy, University of Leipzig, Germany; [2]Center for Biotechnology and Biomedicine, University of Leipzig; [3]Institute of Medical Physics and Biophysics, Medical Faculty, University of Leipzig; [4]Institute of Marine Research, Spanish Council for Scientific Research, (IIM-CSIC), Vigo, Spain; [5]Belarusian State University, Department of Chemistry, Minsk, Belarus
[#] - those authors equality contributed to the study

Running title: *Auto-catalyzed cytochrome c inactivation*

***Thom whom correspondence should be addressed:**
Dr. Maria Fedorova, Institut für Bioanalytische Chemie, Faculty of Chemistry and Mineralogy, Biotechnologisch-Biomedizinisches Zentrum, Leipzig University, Deutscher Platz 5, 04103 Leipzig, Germany. E-mail: maria.fedorova@bbz.uni-leipzig.de.
Dr. Jörg Flemmig, Institute for Medical Physics and Biophysics, Medical Faculty, Leipzig University, Härtelstraße 16 - 18, 04107 Leipzig, Germany. E-mail: joerg.flemmig@medizin.uni-leipzig.de

Keywords: apoptosis, carbonylation, cardolipin, cytochrome c, lipid hydroperoxides, mitochondria, peroxidase activity, proteomics, auto-inactivation, oxidation

Abstract

Cytochrome c (cyt c) is a small hemoprotein involved in electron shuttling in the mitochondrial respiratory chain and is now also recognized as an important mediator of apoptotic cell death. Its role in inducing programmed cell death is closely associated with the formation of a complex with the mitochondrion-specific phospholipid cardiolipin (CL), leading to a gain of peroxidase activity. Yet the molecular mechanisms behind this gain and eventual cyt c auto-inactivation via its release from mitochondria membranes remains largely unknown. Here, we examined the kinetics of the H_2O_2-mediated peroxidase activity of cyt c both in the presence and absence of tetraoleoyl cardiolipin- (TOCL-) and tetralinoleoyl cardiolipin- (TLCL-) () containing liposomes to evaluate the role of cyt c-CL complex formation in the induction and stimulation of cyt c peroxidase activity. Moreover, we examined peroxide-mediated cyt c heme degradation to gain insights into the mechanisms by which cyt c self-limits its-peroxidase activity. Bottom-up proteomics revealed > 50 oxidative modifications on cyt c upon peroxide reduction. Of note, one of these by-products was the Tyr-based "cofactor" trihydroxyphenylalanine quinone (TPQ) capable of inducing deamination of Lys ε-amino groups and formation of the carbonylated product aminoadipic semialdehyde. In view of these results, we propose that auto-induced carbonylation, and thus removal of a positive charge in Lys, abrogates binding of cyt c to negatively charged CL. The proposed mechanism may be responsible for release of cyt c from mitochondrial membranes and ensuing inactivation of its peroxidase activity.

1. Introduction

Cytochrome c (cyt c) was originally identified as an electron shuttle within the respiratory chain, essentially contributing to the aerobic pathway of oxidative phosphorylation. Yet, the single chain hemoprotein is nowadays also known as a key mediator of apoptosis(1), making cyt c an important cornerstone of the cell fate. Upon apoptosis induction the protein is released from the inner-membrane space of the mitochondria to the cytosol where it binds to Apaf-1 (apoptosis activating factor 1)(2) leading to caspase-9 activation(3) and subsequently apoptosis. Thereby cyt c seems actively contributing to this process while the exact biochemical mechanisms for its release from the mitochondria are still under discussion.

Cyt c-mediated pore formation leading to the outer mitochondrial membrane permeabilization was suggested(4), while others did not observe a considerable unfolding and/or insertion of the protein into the outer mitochondrial membrane(5,6). Another mechanism proposed by Kagan et al. links the release of cyt c at the early stage of apoptosis to the gain of a peroxidase activity by this protein(7). Cyt c binds to cardiolipin (CL), a mitochondria-specific phospholipid, which redistributes from the inner to the outer mitochondrial membrane upon apoptosis onset(8-10). This complex formation results in structural modifications of the protein, which trigger a strong peroxidase activity in the presence of H_2O_2(11,12), leading to a specific oxidation of the polyunsaturated fatty acyl chains in CL(7,12,13) thus causing permeabilization of the mitochondrial membrane and the release of cyt c and other pro-apoptotic factors(8,13). Both a cyt c-CL complex formation and a high cyt c-based peroxidase activity were observed during early apoptosis(7). The mitochondrial concentration of H_2O_2 also increases upon apoptosis onset reaching sub-millimolar levels(14). *In vitro* experiments with liposomes confirmed the permeabilization of CL-containing lipid membranes via the described processes(15,16). Thus the formation of cyt C-CL complexes triggers a functional shift of the protein function from electron transport to peroxidase activity(9) which, via CL oxidation, contributes to the intrinsic apoptotic pathway(5,8,17).

As it was highlighted by Kagan et al., the fatty acid composition of CL species influences the binding and subsequent unfolding of cyt c(9). Furthermore, CL acts not only as a passive template for the induction of peroxidase activity in cyt c but actively provides substrates forits enzymatic activity. CL-induced peroxidase activity of cyt c leads to LOOH formation in CL which further promotes its enzymatic activity as well as the subsequent release of cyt c from the mitochondria(7,18). However, it remains to be clarified whether pre-existing lipid hydroperoxides in CL may be sufficient to initiate the proposed auto-catalytic cycle or whether H_2O_2 is still mandatory for the cyt c peroxidase-derived

permeabilization of the mitochondrial membrane upon apoptosis induction(19).

Several studies report an increased degradation of cyt c upon complex formation with CL(20), most likely due to H_2O_2-mediated heme degradation and subsequent iron release(8,21,22). Cyt c oxidative modifications were also observed in the absence of CL after incubating the protein with H_2O_2(21,23). Thereby both, cyt c-derived peroxidase activity and Fenton chemistry were described as possible oxidative pathways, suggesting that peroxidase activity of cyt c and a subsequent heme degradation may be interlinked(24). It remains unclear if CL-dependent degradation of the protein is a result of its peroxidase activity and subsequent heme degradation by released radical by-products.

Here we examined the kinetics of the H_2O_2-mediated peroxidase activity of cyt c both in the absence and presence of CL-containing liposomes to evaluate the role of cyt c-CL complex formation on the induction and promotion of its enzymatic activity. Thereby also the role of the CL fatty acyl chains was considered, thus expanding comparable recent studies(25). Subsequent heme degradation in cyt c was evaluated to gain insights into the self-limiting mechanisms occurring during the cyt c-based peroxidase activity providing basis for free radical chemistry. Furthermore, over 50 oxidative modifications of cyt c resulting from the enzymatic activity of cyt c-CL complexes were studied using a bottom-up proteomics approach and a new mechanism of auto-catalyzed cyt c carbonylation via Tyr derived cofactor leading to the reduction of protein positive charge and dissociation of cyt c -CL complex was proposed.

2. Results

2.1 H_2O_2- and cardiolipin-dependent peroxidase activity of Cytochrome c

We first performed kinetic measurements to investigate cyt c-based peroxidase activity in the sole presence of H_2O_2. The averaged kinetic curves (Fig. 1A) clearly show a time-dependent ABTS radical formation upon addition of increasing H_2O_2 concentrations (straight lines). Three different kinetic phases were observable, namely a lag phase with low enzymatic activity, a subsequent steady-state phase of constant ABTS oxidation followed by a complete cease of the peroxidase activity. Thereby at higher H_2O_2 concentrations (bolder lines) shorter lag phases, higher steady-state enzyme activities and a quicker deactivation of the latter were observed, apparently also leading to lower ABTS radical yields. In the absence of H_2O_2 (dashed line) or cyt c (not shown) no ABTS oxidation took place. Thus H_2O_2 activates and promotes cyt c-based peroxidase activity but subsequently also leads to its auto-catalytic limitation.

A replot of the steady-state ABTS radical formation rate against the applied amount of H_2O_2 (Fig. 1B) showed a linear concentration dependence which indicates pseudo-first order reaction conditions and translates to a k_{obs} value of $6.0 \pm 0.5\ M^{-1}\ s^{-1}$ (Fig. 2B). By comparing the obtained ABTS radical yield to the applied H_2O_2 concentration also the relative efficiency of the cyt c-based peroxidase activity was calculated, again assuming formation of two ABTS radicals per peroxidase cycle. Yet even at 25 µM H_2O_2 only the formation of 20.13 µM ABTS radicals was observed corresponding to a relative yield of 40.3 ± 3.5 %. With increasing hydrogen peroxide concentrations this value considerably decreased (Fig. 1C). Thus a strong H_2O_2-mediated promotion of cyt c-based peroxidase activity translates to lower relative enzymatic efficiencies due to quick enzyme inactivation.

We next tested, whether the presence of CL influences the H_2O_2-dependent peroxidase activity of cyt c by applying LUVs with different lipid compositions. The kinetic measurements (Fig. 2A) clearly showed that both in the absence (black) and in the presence of TOCL-containing liposomes (blue) no cyt c-based peroxidase activity was observed in the absence of H_2O_2 (dashed lines). Yet TOCL strongly promoted the cyt c enzymatic activity in the presence of H_2O_2 (straight lines). A shorter lag phase and an about five-fold higher subsequent H_2O_2-dependent steady-state ABTS radical formation rate (Fig. 2B, $26.7 \pm 1.6\ M^{-}\ s^{-1}$ was observed as compared to the lipid-free samples. Thus, TOCL promotes the H_2O_2-mediated cyt c-based peroxidase activity, which also translates to an about 2.6-fold higher relative product yield (Fig. 2A, 53 µM ABTS radicals).

Upon application of TLCL-containing liposomes (red) cyt c-based peroxidase activity was observed even in the absence of H_2O_2, (Fig. 2A, dashed line), yielding about 20 µM ABTS radicals after 1 h. Moreover, the three kinetic phases described

above were clearly visible. In the additional presence of H_2O_2 (Fig. 2A, straight line) a shorter lag phase, an unchanged subsequent steady-state ABTS radical formation rate and a quicker cease of peroxidase activity were observed, yielding similar overall product yields (22 µM after 40 min). As TLCL does not influence the H_2O_2 concentration-dependent cyt c-based peroxidase activity (Fig. S1), a comparable rate was determined (Fig. 2B, 4.3 ±0.6 M^{-1} s^{-1}) as compared to the lipid-free measurements. Thus TLCL is able to replace H_2O_2 in terms of activation and promotion of cyt c-based peroxidase activity but shows no cumulative effects in the additional presence of H_2O_2.

Control measurements with PLPC-containing liposomes (green) showed no effect of this lipid on the cyt c-based peroxidase activity either in the absence or presence of H_2O_2. This holds for the kinetics of ABTS radical formation (Fig. 2A) as well as for the calculated H_2O_2-dependent steady-state peroxidase activity of cyt c (Fig. 2B, 6.0 ± 1.0 M^{-1} s^{-1}). Thus the reported effects of TOCL and TLCL on cyt c-based peroxidase activity are cardiolipin-specific.

Control measurements were also performed at continuous H_2O_2 production by applying the glucose oxidase (GO) - glucose system. Again the ABTS-based measurements showed sigmoidal kinetics (Fig. S2). Both in the absence of lipid (black) and in the presence of TOCL-containing liposomes (blue) higher constant H_2O_2 production rates translated to shorter lag phases, higher steady-state enzyme activities but also a quicker cease of cyt c-based peroxidase activity. TOCL strongly promoted those effects. Accordingly, in the presence of the lipid about 3.5-fold higher relative enzymatic efficiencies of cyt c were observed as calculated from the amount of ABTS radicals formed after 180 min. However, both in the absence and in the presence of TOCL-containing liposomes the relative product yield again decreased at higher H_2O_2 production rates.

2.2 H_2O_2- and cardiolipin-derived degradation of Cytochrome c

In order to further proof the connection between cyt c-based peroxidase activity and its subsequent inactivation we monitored spectral changes of cyt c upon its incubation with H_2O_2 and/or cardiolipin. The cyt c spectrum (Fig. 3A) clearly showed that in the absence of H_2O_2 (dashed lines) almost no Soret band loss was observed within 3 h of incubation (grey - black), indicating no substantial heme destruction. Yet increasing amounts of H_2O_2 (bolder straight lines) led to a concentration-dependent decrease both of the Soret band at 409 nm and the lower α and β bands beyond 510 nm, indicating heme bleaching. By continuously monitoring the Soret band loss at 409 nm (Fig. 3B), H_2O_2 concentration-dependent sigmoidal curves correlated with the time-dependent peroxidase activity of cyt c (Fig. 1A). In the absence of H_2O_2 (dashed line) no significant Soret band loss was observed.

By replotting the k_{obs} values determined from the linear part of the time-dependent Soret band loss versus used H_2O_2 concentrations, a linear correlation was observed (Fig. 4B, black) and translated to a k_2 value of 0.53 ± 0.01 M^{-1} s^{-1} for the H_2O_2-derived heme destruction in cyt c (Fig. 4C). Control measurements showed a correlation of the H_2O_2-derived Soret band loss (Fig. S3, squares) with the release of free iron (Fig. S3, circles), thus providing another proof for the H_2O_2-derived heme destruction as a cause for the auto-catalytic inactivation of cyt c-based peroxidase activity. Thereby the free iron concentration was determined by repeated sampling and application of the ferrozine assay. The corresponding calibration curve is given as Fig. S4.

Comparable measurements with TOCL-containing liposomes (Fig. 4A, blue) also showed no Soret band loss in the absence of H_2O_2 (dashed line). Yet in its presence (straight line) considerably faster yet only partial heme degradation was observed. Again, a linear correlation between the k_{obs} values (linear part of the kinetics) and the H_2O_2 concentration was determined (Fig. 4B), yielding a k_2 value of 1.58 ± 0.03 M^{-1} s^{-1} (Fig. 4C). Thus, the promoting effect of TOCL on H_2O_2-mediated cyt c-based peroxidase activity (Fig. 2) translates to an about three times faster heme degradation. PLPC (green) did not influence the H_2O_2-derived heme degradation (Fig.4A-C) as the lipid has no effect on cyt c-based peroxidase activity (Fig.2A-B).

The results in the presence of TLCL-containing liposomes (red) were also comparable with the data from the peroxidase activity measurements. Even in the absence of H_2O_2 (Fig. 4A, dashed line) a short lag phase was followed by an exponential loss of the Soret band intensity, indicating heme

destruction in about 77 % of the cyt c proteins. In the additional presence of H_2O_2 (straight line) an instant, even faster and almost complete loss of the Soret band was observed corresponding to the quick deactivation of the cyt c-based peroxidase activity observed under these conditions (Fig. 2). From the replot of the linear part of the Soret band loss against the H_2O_2 concentration, a k_2 value of $2.48 \pm 0.21\ M^{-1}\ s^{-1}$ was calculated, indicating an almost five times faster H_2O_2-derived heme degradation in the presence of TLCL. Thereby the linear relationship is shifted to higher k_{obs} values, illustrating the heme-degrading effect of this lipid in the absence of H_2O_2.

2.3 Effect of cardiolipin-derived lipid hydroperoxides

The results clearly show that TOCL promotes both cyt c-based peroxidase activity (Fig. 2) and subsequent heme degradation (Fig. 4) only in the presence of H_2O_2, while TLCL promotes the named processes even in the absence of H_2O_2. This difference may result from the activation of cyt c-based peroxidase activity by pre-existing lipid hydroperoxides (LOOH) present in TLCL preparations. It is important to note, that TLCL used in the study was derived from the bovine heart preparation and thus contained some amount of endogenously or artificially produced LOOH species (Fig. S5). TLCL-derived lipid peroxides can lead to the formation of further LOOH and, thus, support both peroxidase activity and subsequent heme loss of cyt c in an auto-catalytic fashion. To proof this hypothesis TLCL was pre-incubated with triphenylphosphine (PPh_3) to reduce the LOOH amount before preparing liposomes and performing peroxidase activity measurements and studying heme degradation.

Upon pre-incubation of TLCL (300 µM lipid concentration) with PPh_3 the amount of LOOH was significantly reduced from 2.22 ± 0.24 µM to 0.73 ± 0.11 µM (Fig. S6). As was shown already above non-reduced TLCL (Fig. 5A, red) strongly promoted cyt c-based peroxidase on its own (dashed line) and even more in the presence of H_2O_2 (straight line), as compared to the lipid-free control (black). In contrast, application of reduced TLCL (violet) with or without H_2O_2 supplementation resulted in lower peroxidase activity. Furthermore, higher ABTS radical yields were obtained as compared to non-reduced TLCL, indicating lower levels of heme degradation upon application of the lipid with a reduced LOOH content. These results proof a substantial contribution of LOOH to the self-limiting cyt c-based peroxidase activity.

By monitoring the Soret band loss for non-reduced TLCL (Fig. 5B, red) a complete heme loss was observed within the 3 h measuring time, both in the absence (dashed) and in the presence (straight) of hydrogen peroxide. Upon application of reduced TLCL (violet) heme degradation was partially inhibited, indicating a role of lipid hydroperoxides at peroxidase-derived heme destruction in cyt c. However, still an almost complete heme loss was obtained at the end of the experiment. Most likely the peroxidase activity-mediated auto-catalytic reformation of lipid hydroperoxides in the presence of molecular oxygen keeps the named enzymatic activity running, which, in turn, causes heme degradation and iron release. Indeed, measuring cyt c Soret band loss in the presence of TLCL under hypoxic conditions, a significantly lower rate of heme degradation was observed (Fig. S7), indicating the involvement of oxygen-mediated reactions.

2.4 H_2O_2- and cardiolopin-derived modification of cytochrome c

Previous results clearly demonstrated inactivation of cyt c during peroxidase cycle in the presence of H_2O_2 alone or in combination with cardiolipin. Importantly, TLCL even in the absence of H_2O_2 was capable not only to activate cyt c peroxidase activity but also to induce its inactivation accompanied by heme destruction and subsequent iron release. Cyt c inactivation was proposed to derive from oxidative degradation of the protein by reactive products released during peroxidase cycle. To map oxidative post-translational modifications (oxPTMs) of cyt c (100 µM) incubated alone or in the presence of hydrogen peroxide (1 mM) and/or TLCL (10 mM), we employed gel-based bottom up proteomics approach to monitor over 50 modifications on ten amino acid residues (Table S2). It is important to note that LC-MS/MS based identification of the modification sites performed in this study provided only qualitative results and did not include any quantitative values.

Direct oxidation of Met, Trp, Pro, His, Phe, and Tyr amino acid residues was detected in all studied conditions (Table 1, Table S3). Both Met residues of cyt c (Met 65 and 80) were detected in the form

of methionine sulfoxide. Interestingly, despite the high frequency of peptides carrying Met sulfoxides (especially for Met 65), further oxidation of Met residues to sulfones was not detected. Alternatively, both Cys residues (Cys 14 and 17) were found to be heavily oxidized to sulfonic acid but only in the samples incubated with H_2O_2 (60 min), TLCL (30 and 60 min), and a combination of both (30 and 60 min). No intermediate oxidation states of Cys residues (sulfenic or sulfinic acids) were identified. Single Trp residue in position 59 was oxidized to hydroxyTrp/oxindolylalanine (mass increment of 16 amu relative to unmodified Trp) and dihydroxyTrp/N-formylkynurenine (32 amu) in all samples and no further Trp oxPTMs were detected. Out of four Tyr residues, three (Tyr 48, 67 and 97) were modified to dihydroxyphenylalanine (DOPA; Tyr 48, 67, and 97), DOPA quinone (DQ; Tyr 48 and 67), and trihydroxyphenylalanine (TOPA; Tyr 97). Tyr 74, however, was not detected in any of those three oxidation states. Single oxidation (+ 16 amu) was confirmed for His 33 and Phe 37, 46, and 82 in most of the samples as well. Pro 30, 44, 71 and 76 were found with mass increments of 14 amu (pyroglutamic acid; positions 30, 44, and 76) and 16 amu (Pro 30, 44, 71, and 76). Mass increment of 16 amu on proline residue can correspond either to hydroxylation or carbonylation to glutamic semialdehyde. Protein carbonylation, a well-known oxPTM formed usually via metal catalysed oxidation of Pro, Thr, Arg, and Lys residues, was reported previously for H_2O_2 treated cyt c (25). However, exact confirmation of carbonylated residues using tandem mass spectrometry was not provided so far to the best of our knowledge.

Here, we demonstrated oxidative carbonylation on at least 14 cyt c amino acid residues. Among carbonylated amino acid residues highest number of modified positions was assigned to Lys. Out of 18 Lys residues seven (Lys 39, 53, 55, 72, 73, 79, and 99) were oxidized to aminoadipic semialdehyde. Seven out of eight available Thr were oxidized to 2-amino-3-ketobutyric acid (Thr 19, 28, 40, 49, 58, 63, and 78, but not 102). As mentioned before, for Pro residues both hydroxylation and carbonylation to glutamic semialdehyde result in the same mass increment of 16 amu and thus indistinguishable without carbonyl specific derivatization. Overall, oxidation of Pro with mass increment of 16 amu was detected for all four available Pro residues including Pro 71 (only in TLCL treated samples). Interestingly, none of two Arg residues (positions 38 and 91) have been shown to be carbonylated to glutamic semialdehyde.

2.5 Auto-generated trihydroxyphenylalanine quinone (TPQ) mediated Lys carbonylation.

Tyr residues in cyt c are believed to play an important role not only in cyt c peroxidase catalytic activity but also in peroxidase cycle-induced enzyme inactivation. Several studies proposed formation of Tyr radicals and the presence of diTyr crosslinks in H_2O_2 treated cyt c was confirmed using specific diTyr fluorescence(7,23,26). Based on the mapping of oxidative modifications described above, it was rather surprising that Tyr 74 was not detected in either of the three considered oxidative states (DOPA, DQ, and TOPA). Thus, possibility of diTyr crosslinks formation was further evaluated.

Crosslinked peptides are particularly challenging for the identification using bottom-up proteomics profiling. Indeed, almost no MS/MS based identification of diTyr formation sites are available. Recently, we developed a new MS based approach to localize crosslinked Tyr residues in *in vitro* oxidized human serum albumin using mass increments of *in silico* predicted Tyr containing tryptic peptides as variable modifications to be used in the search engine based identification of diTyr linked sequences (27). This strategy was proven to be successful for cyt c samples as well. Indeed, crosslink peptides representing diTyr formation between Tyr 67 – Tyr 74 were identified in all experimental conditions, whereas peptides crosslinked via Tyr 48 (homodimer) and Tyr 48 – Tyr 74 were present only in the samples incubated with TLCL. These results demonstrated significant involvement of residue at position 74 in Tyr radical-mediated protein crosslinking.

Both Tyr modifications and extensive Lys carbonylation present even in untreated cyt c samples, was rather surprising and suggested a possibility of mechanistic correlation between those two modification types in cyt c.

Taking into account presence of several oxidation states for cyt c Tyr residues accompanied by a high number of carbonylated Lys, we speculated that Lys deamination to carbonyl containing aminoadipic semialdehyde via *in situ* produced

2,4,5-trihydroxyphenylalanine quinone (TPQ) "cofactor", similar to the enzymatic deamination of primary amines described for copper amine oxidase (28), might occur in cyt c under oxidative environment accompanied by the release of a free iron (Fig. S8). To confirm this hypothesis, mass increments corresponding to Tyr oxidation products leading to TPQ formation as well as their amino derivatives were calculated and used as variable modifications for the database search in our experiments. Those included already described Tyr oxPTMs such as diTyr crosslinks, DOPA, TOPA, DQ, as well as new modifications including trihydroxyphenylalanine quinone (TPQ), aminoquinol and iminoquinol. Indeed, analysis of proteomics data resulted in identification of all proposed Tyr PTMs in cyt c samples (Fig. 6). Of course, MS based experiments does not provide full structural assignment of modified residues. However, considering specific elemental composition of modified residues (e.g. $C_9H_{14}N_2O_4$ for aminoquinol as a residue) and derived mass increments relative to Tyr residue (e.g. 33.0215 amu) in combination with high resolution and mass accuracy of Orbitrap mass analyser, our data provide a strong support for the proposed structures.

Thus, considering previously described (section 2.4) and newly considered PTMs, we confirmed modification of Tyr 48 to diTyr (homo- and heterodimer with Tyr 74, both in TLCL containing samples), DOPA (all incubations), DQ (H_2O_2, TLCL, and combination of both), TPQ (all conditions), aminoquinol (all conditions), and iminoquinol (TLCL with and without H_2O_2) (Fig. 6) Examples of tandem mass spectra of TPQ, amino- and iminoquinol modified Tyr 48 containing peptides are shown on Fig. S9. Furthermore, relative label free quantification of Tyr 48 containing peptides demonstrated their presence mostly in H_2O_2 and TLCL treated samples (Fig. S10).

In contrast, Tyr 67 was detected only in the form of diTyr (heterodimer with Tyr 74; all conditions), DOPA (all conditions), and DQ (control, H_2O_2, TLCL+ H_2O_2 samples). Tyr 74 was identified in the form of diTyr crosslinks (heterodimers with Tyr 67 in all conditions and with Tyr 48 for TLCL samples), TPQ (H_2O_2, TLCL, and combination of both), as well as aminoquinol (all conditions) and iminoquinol (H_2O_2, TLCL, and combination of both). Finally, Tyr 97 was detected in modified form only in H_2O_2 and TLCL containing samples, including DOPA (TLCL+ H_2O_2), TOPA (only TLCL and TLCL+ H_2O_2), and aminoquinol (H_2O_2, TLCL, and combination of both).

Overall, each Tyr residues showed certain specificity in terms of oxPTMs as well as sample treatment types, with general tendency for TPQ and iminoquinol to be present in H_2O_2 containing samples independent of the presence of TLCL, with Tyr 48 and 74 showing the highest coverage of oxPTM along the whole proposed pathway (Fig. 6).

2.6 Cytochrome c modifications by electrophilic lipid peroxidation products

Finally, we investigated cyt c adducts between nucleophilic amino acid residues (Lys, Arg, His, Cys) and electrophilic lipid peroxidation products (LPP), including low molecular weight aldehydes such as acrolein, glyoxal, and methylglyoxal as well as well-known α,β-unsaturated aldehydes, hydroxy- and oxo-nonenals (HNE and ONE), formed by a β-scission of ω-6 PUFA at C9 position. As expected, HNE and ONE Michael adducts were identified only in the samples co-incubated with TLCL. In total four modification sites were identified including Lys 5 (ONE), His 33 (ONE and HNE), Lys 39 (ONE), and Lys 99 (ONE).

Adducts with glyoxal and acrolein were confirmed for His 26, Lys 27, His 33, Lys 39, Lys 53, Lys 72, Lys 86, Lys 88, Arg 91, and Lys 100. Majority of the modifications were identified in TLCL treated samples, however carboxymethyl Lys was identified at the positions 39, 53 and 88 even in the sample not exposed to TLCL during the experiments. Taking into account that cyt c used in the study derived from a bovine heart preparation, these modifications might be either present in the original sample or derived from co-purified lipids after oxidant exposure.

2.7 Comparison of cytochrome c modifications in the presence of H_2O_2 and/or TLCL

Comparing oxidation sites between different samples, it can be seen that most of the oxPTMs were detectable already in untreated samples (control 0, 30 and 60 min incubation) (Fig. 7A). Once more, it is important to note that LC-MS/MS based identification of modification sites performed in this study provided only qualitative results and did not include any quantitative values.

Interestingly, residues in the middle of cyt c sequence (Fig. 7B) were oxidized in most of the samples independent of the treatment conditions (Thr 28, Pro 30, His 33, Phe 36, Lys 39, Thr 40, Pro 44, Tyr 48, Thr 49, Lys 53, Thr 58, Trp 59, Met 65, Tyr 67, Pro 76, Met 80). Oxidation of Cys 14 and 17 to sulfonic acid occurred only in the samples treated with H_2O_2, TLCL and combination of both, indicating significant conformational changes in cyt c heme coordinating pocket in conditions promoting peroxidase activity and protein inactivation (Fig. 7, A-D). Additionally, specific oxidation induced in the presence of H_2O_2 and TLCL included carbonylation of Thr 19 and Lys 79, as well as carboxymethyl adduct on Lys 88. Furthermore, several sites specific oxidative PTMs were detected only in the samples treated with TLCL alone or in the presence of H_2O_2 (His 26, crosslinks between Tyr 48 – Tyr 48, Tyr 48 – Tyr 74, Pro 71, and Lys 99; Fig. 7, C-D). Interestingly, the presence of H_2O_2 in TLCL treated samples did not result in any additional modification indicating absence of cumulative effect between lipid and hydrogen peroxide exposure.

2.8 Cyt c carbonylation reduced its ability to bind CL

To demonstrate that cyt c carbonylation attenuates its binding to CL, extent of cyt c carbonylation upon H_2O_2 treatment was relatively quantified using cyt c labeling with carbonyl reactive fluorescent dye 7-(diethylamino)-coumarin-3-carbohydrazide (CHH) (Fig. 9 and S11A). Cyt c incubation with hydrogen peroxide for 30 and 60 min resulted in more than threefold increase of total protein carbonyls. Using reversed-mode native PAGE we demonstrated significant reduction in cyt c positive net charge upon oxidation, proportional to the increase of cyt c carbonylation signal (Fig. 9 and S11B).

Furthermore, using competitive binding assay utilizing nonyl acridine orange (NAO), we determined decrease in binding of CL and cyt c upon oxidation (Table 2). Thus, CL-cyt c binding constant (K_b) for control protein sample as well as cyt c incubated for 30 and 60 min in the absence of H_2O_2, was estimated as 15×10^7 M^{-1}. Incubation with hydrogen peroxide for 30 and 60 min lead to the significant decrease of K_b values (threefold), providing clear correlation between cyt c carbonylation, associated decrease of protein positive charge and its ability to bind to CL.

3. Discussion

Recently, cyt c received a lot of scientific attention due its role in apoptosis associated with cyt c release in cytoplasm and caspase activation. Cyt c forms a complex with the mitochondria specific lipid cardiolipin which, upon oxidation, leads to the detachment of the protein from the inner mitochondria membrane, permeabilization of outer membrane and subsequent release of cyt c to the cytoplasm (29). During this pathway, cyt c gains a peroxidase function, utilizing H_2O_2 and lipid-derived peroxides as substrates. However, the exact mechanism of transition of cyt c from low to high peroxidase state remains elusive. To address, at least partially, this question we used the combination of biochemical methods with bottom-up proteomics for identification of cyt c oxidative post-translational modifications (oxPTMs). Recently, a role of H_2O_2-mediated oxPTMs in the promotion five-coordinated heme state of cyt c during pre-catalytical lag-phase was proposed (30). Indeed, higher H_2O_2 concentrations resulted in a shorter lag-phase, consistent with the idea of faster oxidation rates of cyt c in the presence of high oxidant concentrations. TOCL promoted cyt c peroxidase activity, leading to the shorter lag-phase and also faster enzyme inactivation. Electrostatic interactions between positively charged residues of cyt c and negatively charged phosphate groups of CL are essential to cyt c - CL complex formation and believed to be a primary driving force in respect to hydrophobic interaction and hydrogen bonding. Recently it was demonstrated that several sites on cyt c are engaged into CL-cyt c interactions governed by electrostatic forces (31). It was proposed that sites A and L, although located at the opposite end of the protein, can be seen as a joint binding site containing hydrophobic and positively charged residues. Binding via such not contiguous site results in opening of heme pocket via membrane pulling and thus promote cyt c peroxidase activity.

Interestingly, TLCL alone in the absence of H_2O_2 also resulted in activation of peroxidase activity, which we showed to be dependent on the presence of LOOH in TLCL preparations. Apparently, combined effect of structural remodeling of cyt c

via CL-cyt c complex formation and the presence of initially low levels of organic peroxides was sufficient to initiate peroxidase cycle. We propose that high levels of TLCL-mediated peroxidase activity, despite low level of initial LOOH (2.2 μM) as an initial substrate, can be explained by continuous LOOH production from native TLCL via free radicals generated as a by-products of peroxidase cycle (Fig. 8, red route). *In situ* LOOH production results in continuous substrate supply, thus fueling the peroxidase cycle, producing new radicals and creating a closed loop responsible for the fast enzyme inactivation. Indeed upon removal of LOOH, peroxidase activity of cyt c-TLCL closely resemble TOCL curve. Interestingly, we do not observe cumulative effect between non-reduced TLCL and H_2O_2 on reaction kinetics and TLCL alone was capable to stimulate fast cyt c inactivation and degradation.

The majority of the studies on the role of cyt c -CL complex and its peroxidase activity have been focused on CL oxidative modifications associated with the changes in mitochondria membrane properties leading to its permeabilization (7), leaving the significance of cyt c oxPTMs for complex formation, peroxidase activity initiation as well as cyt c dissociation from membranes often overlooked. Here, to follow up on observed changes in reaction kinetics, we monitored multiple oxPTMs of cyt c in the absence or presence of H_2O_2, TLCL and combination of both. In all studied conditions we observed a high number of oxidative modifications covering the middle part of cyt c sequence. However, heme-region amino acids were not significantly modified unless severe treatment was applied. Tyr residues and their PTMs are usually found to be relevant in peroxidase activity of classical enzymes as well as cyt c peroxidase (25). Role of Tyr residues in peroxidase cycle are usually associated with the formation of Tyr radicals via one-electron reduction of Compound I to Compound II. Tyr radical formation is often followed by its recombination to the corresponding dityrosine cross-links (23), however the exact localization of PTM sites was never provided before. Here we detected three different types of diTyr cross-links in cyt c involving Tyr 48, 67, and 74. Tyr 67 hydrogen bond network is essential for heme coordination and tyrosine may also serve as electron donor upon Compound I to Compound II one-electron reduction (Fig. 8, green route). Furthermore, our results indicate significant involvement of Tyr 74 in this process, since only diTyr hetero- but not homodimers between Tyr 67 and Tyr 74 were identified. Interestingly, involvement of Tyr 48, another surface exposed residue, in Tyr radical mediated diTyr crosslinks was evident only in TLCL containing samples. It is interesting to note, that cyt c Tyr residues are known to be involved in the regulation of apoptosis via other type of regulatory PTMs, namely phosphorylation and nitration. Thus, Tyr 48 phosphorylation was shown to possess anti-apoptotic properties by impairing Apaf-1 mediated activation of caspase 9 (32). Although the direct role of Tyr oxidation in regulation of apoptotic signaling is not fully understood, Tyr 48 present in oxidized form would be unavailable for phosphorylation, thus limiting anti-apoptotic function of this modification via PTM cross-talk.

One of the most abundant oxidative modifications of cyt c was carbonylation. Cyt c carbonylation upon incubation with H_2O_2 was already demonstrated by oxyblot (23). Recently, H_2O_2-induced carbonylation of Lys 72 and 73 during initial lag-phase of cyt c peroxidase catalysis was proposed as a mechanism of pre-catalyst activation (23). Despite detecting carbonylated cyt c proteoforms authors, however, did not provide any confirmation of proposed modification sites. Here, we detected 14 carbonylation sites including seven Lys and seven Thr residues. Such a large number of carbonylation sites made us wonder if it can mechanistically correlate with cyt c peroxidase activity and subsequent radicals formation. Keeping in mind high involvement of Tyr residues and Tyr-derived PTMs in peroxidase cycle, as well as known reaction mechanisms of Lys carbonylation (33), the analogy with the copper-containing enzyme lysyl oxidase (LOX), responsible for Lys deamination to aminoadipic semialdehyde in extracellular matrix proteins, first came to mind. Yet, instead of LOX lysine tyrosyl quinone (LTQ) cofactor we proposed the formation of 2,4,5-trihydroxyphenylalanine quinone (TPQ), previously described for a copper amine oxidase catalysing deamination of primary amines (23). Applying these reaction mechanisms to Tyr residues in cyt c, we monitored formation of corresponding TPQ, aminoquinol and iminoquinol PTMs. Indeed, both surface exposed Tyr 48 and 74.

Detection of amino and imino group containing derivatives of cyt c Tyr residues allows to propose that auto-generated TPQ "cofactors" in cyt c can mediate Lys deamination to observed aminoadipic semiladehydes on Lys 39, 53, 55, 72, 73, and 99. Interestingly, out of 18 Lys residues only seven positions were identified in the form of aminoadipic semialdehyde. Furthermore, carbonylated Lys residues are mainly located in the site A and contribute to cyt - CL complex formation via electrostatic interactions.

Cyt c is rich in Lys residues, which represent 17 % of its sequence vs 6 % average Lys abundance in mammalian proteomes. Many Lys residues in cyt c participate in its interaction with lipid membranes and protein binding partners (30). Our and previously published data indicate high susceptibility of cyt c Lys residues to a variety of modifications each of which can potentially change protein net charge and thus interaction surfaces for the binding partners. Indeed, co-incubation of cyt c with HNE resulted in a shift of the protein pI from 9.7 to 9.25 (34). Furthermore, using site directed mutagenesis it was demonstrated that substitution of Lys 72 and 73 with Asn cancels CL - cyt c binding and CL-induced peroxidase activity whereas Lys to Arg mutations at the same sites permit cyt c - CL interactions (35). We demonstrated that cyt c carbonylation was associated with the loss of protein positive charge and resulted in a significantly lower binding constants with CL-containing liposomes, conforming one more time the importance of Lys residues in establishment of electrostatic interaction between the cyt c and cardiolipin. Thus, it is tempting to speculate that similar to the well-studied histone PTM code maintained via methylation of Lys-rich protein tails, cyt c Lys PTMs, formed via auto-generated TPQ-mediated deamination, lead to the elimination of the positive charge and might be seen as a regulatory mechanism responsible for the switch of cyt c interaction partners (e.g. ETC proteins, anionic lipids, or membrane detachment) and thus regulating its moonlighting nature or functional switch.

4. Experimental procedures

4.1 Materials

If not otherwise stated the chemicals were obtained at the highest available purity from Sigma-Aldrich (Merck KGaA, Darmstadt, Germany) or Fluka (Honeywell GmbH, Offenbach, Germany) and were used without further purification. Cytochrome c (cyt c) from bovine heart (C3131, 95 % purity), glucose oxidase (GO, G6137, > 300 U/mg), horseradish peroxidase (HRP, P6782, > 1000 U/mg), acridine orange 10-nonyl bromide (nonyl acridine orange, NAO), diethylenetriaminepentaacetic acid (DTPA), and 7-(diethylamino)coumarin-3-carbohydrazide (CHH) were obtained from Sigma-Aldrich. The concentration of cyt c was repeatedly checked by performing UV-Vis spectroscopy using the Soret band absorption measurement (ε_{408} = 1.04 x 10^5 M^{-1} s^{-1}) (36). H_2O_2 stock solutions were freshly prepared from a 30 % stock by diluting in bi-distilled H_2O, H_2O_2 concentration was determined spectroscopically at 230 and 240 nm (ε_{240} = 74 M^{-1} cm^{-1}, ε_{230} = 43.6 M^{-1} cm^{-1}) and solutions were stored at 4 °C till usage (37,38). Acetonitrile and formic acid were purchased from Biosolve (Valkenswaard, Netherlands). SDS, glycerol, and dithiothreitol (DTT) were obtained from Carl Roth GmbH + Co. KG (Karlsruhe, Germany). Trypsin and Coomassie® Brilliant Blue G-250 were purchased from Serva Electrophoresis GmbH (Heidelberg, Germany).

All lipids used in the study were obtained from Avanti® Polar Lipids, Inc, Alabaster, AL, USA. Briefly, 1,2-dioleoyl-*sn*-glycero-3-phosphocholine (DOPC), 1-palmitoyl-2-linoleoyl-*sn*-glycero-3-phosphocholine (PLPC), 1-palmitoyl-2-oleoyl-*sn*-glycero-3-phosphoethanolamine (POPE), tetralinoleoyl cardiolipin (TLCL, bovine heart) and tetraoleoyl cardiolipin (TOCL) were used for the liposome preparation. Thereby, if not otherwise stated, the following molar compositions were used: DOPC/PLPC 2:3, DOPC/TOCL 7/3 and DOPC/TLCL/POPE 5/3/2, meaning a cardiolipin concentration of 30 mol % in the corresponding liposomes.

4.2 Liposome preparation

Large unilamellar liposomes (LUVs) were prepared by extrusion (22,39). Briefly, single lipid stock solutions (10 mg/mL in chloroform) were

mixed and evaporated in a vacuum centrifuge (Vacuum Concentrator Centrifugal Evaporator R 10.22, Jouan, Fisher Scientific GmbH, Schwerte, Germany), and obtained lipid film was dissolved in phosphate buffer (PB, 10 mM, pH 7.4) (for UV-Vis spectroscopy) or ammonium bicarbonate buffer (ABC, 50 mM, pH 7.8) (for gel electrophoresis, mass spectrometry) by thorough vortexing. The resulting multilamellar vesicles were extruded 19 times through an hydrophilic polycarbonate filter (Merck Millipore, Merck Chemicals GmbH, Darmstadt, Germany, 25 mm diameter, 0.1 µm pore size) in a mini extruder (Avanti® Polar Lipids, Inc, Alabaster, AL, USA). LUVs size distribution was determined by nanoparticle tracking analysis (NTA) using a NanoSight LM20 Nanoparticle Analysis System (NanoSight, Amesbury, United Kingdom), equipped with a 650 nm laser. For each sample three measurements (60 s each) at 23.3 °C were performed, using a concentration of 10^7 - 10^9 particles/ml. The lipid composition and size of the liposomes applied in the experiments are given in Table S1 whereby the most common lipid compositions are shown italic.

4.3 Lipid quantification

Lipid concentration in the extruded samples was determined by Bartlett assay (40) with slight modifications (41). Briefly, liposomes were incinerated in $HClO_4$ (70 %, v/v, 90 min, 230 °C), ascorbic acid (700 µL, 3 %, v/v) and ammonium molybdate solution (700 µL, 3.6 mM, v/v, 12.5 % perchloric acid) were added and samples were incubated for 5 min at 100 °C. The concentration of ammonium phosphomolybdate complexes was determined spectroscopically (Tecan Infinite 200 Pro, Männedorf, Switzerland) at 830 nm by comparing to a calibration curve prepared with 6.4 - 64 nmol NaH_2PO_4.

4.4 Lipid hydroperoxide reduction

For selected experiments lipid hydroperoxides (LOOH) in the LUVs were reduced by incubating the chloroform stock solution of the lipid mixture (DOPC/TLCL 7/3) with triphenylphosphine (PPh_3, 2 mM chloroform) for 1 h at 30 °C in the dark (42). Chloroform was evaporated and liposomes were prepared as described above. The amount of lipid hydroperoxides before and after PPh_3 reduction was determined by monitoring the enzymatic activity of HRP (0.1 µM) in the presence of ABTS (2,2'-azino-bis(3-ethylbenzothiazoline-6-sulphonic acid, 1 mM) in 1 mM liposomes and comparing the obtained values to the ABTS oxidation rates observed in the presence of H_2O_2.

4.5 Peroxidase activity measurements

If not stated otherwise, samples for the peroxidase measurements were prepared in 96-well plates, containing cyt c (5 µM), liposomes (500 µM lipid concentration) and ABTS (1 mM) in PB. After pre-incubation for 5 min at 37 °C, H_2O_2 (up to 500 µM) was added by using an injector device of the plate reader (Tecan Infinite 200 Pro, Männedorf, Switzerland) and the formation of $ABTS^{\bullet+}$ was followed by absorbance measurement at 734 nm (ε_{734} = 1.5 x 10^4 M^{-1} s^{-1}) (43) at 37 °C for up to 3 h. From the linear range of absorbance increase curves, the initial ABTS oxidation rate was determined (5).

Selected experiments were also performed in the presence of glucose oxidase (GO) and glucose as a continuous H_2O_2-producing system (21,44). Briefly, samples were prepared as described above in the additional presence of GO (up to 4.70 mU) and pre-incubated for 5 min at 37 °C. Glucose (1 mM) was added using the injector device of the plate reader. H_2O_2 production rates were adjusted by applying different amounts of GO (0.24 - 4.70 mU). Calibration curve obtained from control measurements with HRP (0.1 µM), ABTS (1 mM), glucose (1 mM) and using different GO concentrations was consulted.

4.6 Heme degradation measurements

Cyt c (5 - 30 µM) was incubated with an up to 100-fold excess of H_2O_2 either in the absence or presence of an 100-fold lipid excess in PB (10 mM, pH 7.4). Spectral changes between 380 nm and 580 nm were followed at 37 °C for 3 h. From the absorbance loss at 408 nm (Soret peak) (21,36) k_{obs} values were calculated by plotting the linear part of the Soret band loss kinetics against the applied H_2O_2 concentration. From the slope of these plots k_2 values were calculated by considering the applied cyt c concentration.

Selected experiments were also performed to correlate (21) the Soret band loss with the release of iron from cyt c, by applying the ferrozine assay(21,45) with slight modifications (46,47). Briefly, cyt c (30 µM) was pre-incubated in PB

(10 mM, pH 7.4) at 37 °C. H_2O_2 (3 mM) was added by using the injector device of the plate reader. The Soret band loss was followed at 408 nm for up to 3 h. Ascorbic acid (150 mM) were added to selected wells at fixed time points via the injector device of the reader to stop the reaction and reduce iron to the ferrous state. After completion of the absorbance measurements, parts of the samples were transferred either to a well containing ferrozine (2.5 mM, monosodium salt hydrate of 3-(2-pyridyl)-5,6-diphenyl-1,2,4-triazine-*p,p'*-disulfonic acid; in 8 % ammonium acetate solution) or to a well containing PB. The absorbance was measured at 562 nm (46), using the second well for zero compensation. The free iron concentration in the samples was determined by comparing the obtained net absorbance to a calibration curve generated with ferrozine and $FeCl_3$ under the same experimental conditions.

To monitor cyt c heme degradation at normoxic and hypoxic conditions, TLCL liposomes (1.5 mM in 10 mM PB) were prepared as stated above and incubated with cyt c (15 µM) in PB in a Hellma Precision cell Suprasil® cuvette. For normoxic conditions, the decrease of the Soret band (408 nm) absorbance was monitored over 90 min at 37 °C. For hypoxic measurements, PB was sonicated (10 min, RT), PB and cyt c stock solutions were degassed by vacuum application in an Eppendorf Concentrator (10 min, RT) and purged with nitrogen (10 min, RT), before measurements of Soret band absorbance carried out in a nitrogen flushed air tight screw cap Hellma Precision cell Suprasil® cuvette.

4.7 SDS PAGE and in-gel digestion

Cyt c (100 µM) was incubated in the absence or presence of TLCL-containing liposomes (10 mM) and H_2O_2 (1 mM) in ABC buffer at 37 °C for 30 or 60 min. Samples were extracted using tert-butyl methyl ether (MTBE) protocol (48). Briefly, 350 µL of methanol and 1250 µL of MTBE were added, followed by 10 s vortexing after each step. The mixture was left on a rotating shaker for 1 h at 4 °C. To induce phase separation, 313 µL of deionized water was added. Samples were left on a rotary shaker for additional 10 min and centrifuged for 10 min at 1000 x g. The upper phase was removed and the lower aqueous phase together with protein precipitate was dried in the vacuum centrifuge for protein analysis. Dried samples were dissolved in Laemmli sample buffer (62.5 mM Tris, 2.5 % (w/v) SDS, 0.2 % (w/v) bromphenol blue, 5 % β-mercaptoethanol, 10 % (w/v) glycerol, pH 6.8), separated by SDS-PAGE (18 % T, 1 mm) and stained with Coomassie® Brilliant Blue G-250. Visible protein lanes were cut out, de-stained with acetonitrile (50 %, v/v, in 50 mM NH_4HCO_3), centrifuged (1 h, 37 °C, 750 rpm), dehydrated with 100 % acetonitrile and dried by vacuum concentration. Proteins were digested with trypsin (375 ng in 3 mM in ABC, 4 h, 37 °C, 550 rpm) and peptides were extracted using consecutive incubations with 100 %, 50 % and 100 % acetonitrile (15 min sonication for each step). Combined extracts were vacuum-concentrated and stored at -20 °C. Before MS analysis, peptides were dissolved in 10 µL 60 % aqueous acetonitrile containing 0.5% formic acid and further diluted 1:20 with 3 % aqueous acetonitrile.

4.8 LC-MS/MS of tryptic peptides

A nano-Acquity UPLC (Waters GmbH, Eschborn, Germany) was coupled online to an LTQ Orbitrap XL ETD mass spectrometer equipped with a nano-ESI source (Thermo Fischer Scientific, Bremen, Germany). Eluent A was aqueous formic acid (0.1%, v/v), and eluent B was formic acid (0.1%, v/v) in acetonitrile. Samples (10 µL) were loaded onto the trap column (nanoAcquity symmetry C18, internal diameter 180 µm, length 20 mm, particle diameter 5 µm) at a flow rate of 10 µL/min. Peptides were separated on BEH 130 column (C18-phase, internal diameter 75 µm, length 100 mm, particle diameter 1.7 µm) with a flow rate of 0.4 µL/min using two step gradients from 3 to 30 % eluent B over 18 min and then to 85 % eluent B over 1 min. After an equilibration time of 12 min samples were injected every 33 min.

The transfer capillary temperature was set to 200 °C and the tube lens voltage to 120 V. An ion spray voltage of 1.5 kV was applied to a PicoTip online nano-ESI emitter (New Objective, Berlin, Germany). The precursor ion survey scans were acquired at an orbitrap (resolution of 60,000 at *m/z* 400) for a *m/z* range from 400 to 2000. CID-tandem mass spectra (isolation width 2, activation Q 0.25, normalized collision energy 35 %, activation time 30 ms) were recorded in the linear ion trap by data-dependent acquisition (DDA) for the top six most abundant ions in each survey scan with dynamic exclusion for 60 s using Xcalibur

software (version 2.0.7). Peptides were identified using Sequest search engine (Proteome Discoverer 1.4, Thermo Scientific) against Uniprot database, allowing up to two missed cleavages and a mass tolerance of 10 ppm for precursor ions and 0.8 Da for product ions. The list of variable modifications used for database search is provided in Table S2. Results were filtered for rank 1 high confidence peptides and score vs. charge states corresponding to Xcorr/z 2.0/2, 2.25/3, 2.5/4, 2.75/5.

4.9 Shotgun MS analysis of lipid hydroperoxides

Dried lipid-containing MTBE extracts were dissolved in ESI solution (methanol:chloroform, 2:1 v/v, containing 5 mM ammonium formate), and analyzed by direct infusion (15 µL) using robotic nanoflow ion source TriVersa NanoMate (Advion BioSciences, Ithaca NY) and nanoelectrospray chips (1.4 kV ionization voltage, 0.4 psi nitrogen backpressure) coupled to an LTQ Orbitrap XL ETD mass spectrometer (Thermo Fischer Scientific GmbH, Bremen, Germany) operated in negative ion mode. Transfer capillary temperature was 200 °C and the tube lens voltage was set to -120 V. Mass spectra were acquired with a target mass resolution of 100 000 at *m/z* 400 in the Orbitrap mass analyzer. Tandem mass spectra (MS/MS) were acquired in the linear ion trap (LTQ) using an isolation width of 1.5 Da and normalized collision energy (nCE) of 35 %. Data were analyzed manually by using the XCalibur software (2.07, Thermo Fisher Scientific, San Jose, CA, USA).

4.10 Cyt c carbonylation analysis using CHH derivatization

Cyt c (100 µM) in phosphate buffer (50 mM, pH 7.0) was incubated with or without H_2O_2 (1 mM, 37°C) for 0, 30 and 60 min. Reactions were stopped by ultrafiltration (Vivaspin™ 2 ultrafiltration devices with 5000 MW cut off polyethersulphone filter, Sartorius AG, Hannover, Germany) and protein concentration in recovered solutions was determined by Bradford assay (49). Cyt c (0.4 µM) was incubated with 7-(diethylamino)coumarin-3-carbohydrazide (CHH; 150 µM, 2 h, 37°C), and separated by SDS-PAGE (12% T) (50). Gels were washed twice with water (10 min) and visualized on a ChemiDoc™ MP (Bio-Rad Laboratories GmbH, München, Germany), using the Image Lab™ software and DyLight 488 channel filter for Blue Epi illumination. Images were quantified using ImageJ.(51)**.**

Reduction of cyt c positive charge upon oxidation was studied using native PAGE (7.5% T) separation performed in reverse electrophoresis mode(52)**.** Resulting gels were stained with Coomassie, images were acquired on a ChemiDoc™ MP (Bio-Rad Laboratories GmbH, München, Germany) and quantified using Image J.

4.11 Cyt c -CL binding assay

Large unilamellar liposomes of POPC (5 mM) or POPC/TLC mixture (2.5 mM each) were prepared in phosphate buffer (50 mM, pH 7) containing 100 µM DTPA by extrusion as described in section 4.2. Liposomes (1 mM of total lipid) were incubated with cyt *c* (20 µM; 30 min, RT), afterwards acridine 10-nonyl bromide (NAO; 4 mM, 1:4 ratio lipid:NAO) was added and mixtures were incubated for 1 h (RT). 10 µL of each sample was separated by native PAGE (7.5% T) in the reverse electrophoresis mode. The fluorescence of NAO was monitored at 520 nm using ChemiDoc™ MP (Bio-Rad Laboratories GmbH, München, Germany). Binding constants were calculated according to Belikova et al (52).

Acknowledgment

We thank Prof. Ralf Hoffmann (Institute of Bioanalytical Chemistry, University of Leipzig) for providing access to his laboratory and mass spectrometers. Financial support from the German Federal Ministry of Education and Research (BMBF) within the framework of the e:Med research and funding concept for SysMedOS project is gratefully acknowledged. We acknowledge financial support from the Deutsche Forschungsgemeinschaft (DFG; FE-1236/3-1 to M.F.), and the European Regional Development Fund (ERDF, European Union and Free State Saxony; 100146238 and 100121468 to M.F). Xunta de Galicia is thankfully acknowledged for the postdoctoral scholarship provided L.M.

Conflict of Interest

The authors declare that they have no conflicts of interest with the content of this article.

Author Contributions

UB, JA, JF, OIS, MF contributed to the idea conception and experimental design. UB performed all experiments. ML performed TLCL-cyt c peroxides activity experiments under oxygen and nitrogen atmosphere. ML and LM performed cyt c carbonylation and CL binding assays. JF supervised and performed all data analysis for all biochemical experiment. MF supervised and performed all data analysis for all proteomics and lipidomics experiments as well as cyt c carbonylation and CL binding assays. The manuscript was written through the contributions of all authors (UB, ML, JA, JF, OIS, MF). All authors have given approval to the final version of the manuscript.

References

1. Liu, X., Kim, C. N., Yang, J., Jemmerson, R., and Wang, X. (1996) Induction of apoptotic program in cell-free extracts: requirement for dATP and cytochrome c. *Cell* **86,** 147-157
2. Mignotte, B. and Vayssiere, J. L. (1998) Mitochondria and apoptosis. *Eur. J. Biochem.* **252,** 1-15
3. Garcia-Heredia, J. M., Diaz-Moreno, I., Nieto, P. M., Orzaez, M., Kocanis, S., Teixeira, M., Perez-Paya, E., Diaz-Quintana, A., and De la Rosa, M. A. (2010) Nitration of tyrosine 74 prevents human cytochrome c to play a key role in apoptosis signaling by blocking caspase-9 activation. *Biochim. Biophys. Acta.* **1797,** 981-993
4. Bergstrom, C. L., Beales, P. A., Lv, Y., Vanderlick, T. K., and Groves, J. T. (2013) Cytochrome c causes pore formation in cardiolipin-containing membranes. *Proc. Natl. Acad. Sci. U. S. A.* **110,** 6269-6274
5. Mandal, A., Hoop, C. L., DeLucia, M., Kodali, R., Kagan, V. E., Ahn, J., and van der Wel, P. C. (2015) Structural changes and proapoptotic peroxidase activity of cardiolipin-bound mitochondrial cytochrome c. *Biophys. J.* **109,** 1873-1884
6. Pandiscia, L. A. and Schweitzer-Stenner, R. (2015) Coexistence of native-like and non-native partially unfolded ferricytochrome c on the surface of cardiolipin-containing liposomes. *J. Phys. Chem. B.* **119,** 1334-1349
7. Kagan, V. E., Tyurin, V. A., Jiang, J., Tyurina, Y. Y., Ritov, V. B., Amoscato, A. A., Osipov, A. N., Belikova, N. A., Kapralov, A. A., Kini, V., Vlasova, I. I., Zhao, Q., Zou, M., Di, P., Svistunenko, D. A., Kurnikov, I. V., and Borisenko, G. G. (2005) Cytochrome c acts as a cardiolipin oxygenase required for release of proapoptotic factors. *Nat. Chem. Biol.* **1,** 223-232
8. Ascenzi, P., Coletta, M., Wilson, M. T., Fiorucci, L., Marino, M., Polticelli, F., Sinibaldi, F., and Santucci, R. (2015) Cardiolipin-cytochrome c complex: Switching cytochrome c from an electron-transfer shuttle to a myoglobin- and a peroxidase-like heme-protein. *IUBMB Life* **67,** 98-109
9. Kagan, V. E., Bayir, H. A., Belikova, N. A., Kapralov, O., Tyurina, Y. Y., Tyurin, V. A., Jiang, J., Stoyanovsky, D. A., Wipf, P., Kochanek, P. M., Greenberger, J. S., Pitt, B., Shvedova, A. A., and Borisenko, G. (2009) Cytochrome c/cardiolipin relations in mitochondria: a kiss of death. *Free Radic. Biol. Med.* **46,** 1439-1453
10. Hüttemann, M., Pecina, P., Rainbolt, M., Sanderson, T. H., Kagan, V. E., Samavati, L., Doan, J. W., and Lee, I. (2011) The multiple functions of cytochrome c and their regulation in life and death decisions of the mammalian cell: From respiration to apoptosis. *Mitochondrion* **11,** 369-381
11. Belikova, N. A., Vladimirov, Y. A., Osipov, A. N., Kapralov, A. A., Tyurin, V. A., Potapovich, M. V., Basova, L. V., Peterson, J., Kurnikov, I. V., and Kagan, V. E. (2006) Peroxidase activity and structural transitions of cytochrome c bound to cardiolipin-containing membranes. *Biochemistry.* **45,** 4998-5009
12. Basova, L. V., Kurnikov, I. V., Wang, L., Ritov, V. B., Belikova, N. A., Vlasova, I. I., Pacheco, A. A., Winnica, D. E., Peterson, J., Bayir, H., Waldeck, D. H., and Kagan, V. E. (2007) Cardiolipin switch in mitochondria: shutting off the reduction of cytochrome c and turning on the peroxidase activity. *Biochemistry.* **46,** 3423-3434
13. Patriarca, A., Eliseo, T., Sinibaldi, F., Piro, M. C., Melis, R., Paci, M., Cicero, D. O., Polticelli, F., Santucci, R., and Fiorucci, L. (2009) ATP acts as a regulatory effector in modulating structural transitions of cytochrome c: implications for apoptotic activity. *Biochemistry.* **48,** 3279-3287
14. Giorgio, M., Trinei, M., Migliaccio, E., and Pelicci, P. G. (2007) Hydrogen peroxide: a metabolic by-product or a common mediator of ageing signals? *Nat. Rev. Mol. Cell Biol.* **8,** 722-728
15. Firsov, A. M., Kotova, E. A., Korepanova, E. A., Osipov, A. N., and Antonenko, Y. N. (2015) Peroxidative permeabilization of liposomes induced by cytochrome c/cardiolipin complex. *Biochim. Biophys. Acta.* **1848,** 767-774
16. Firsov, A. M., Kotova, E. A., Orlov, V. N., Antonenko, Y. N., and Skulachev, V. P. (2016) A mitochondria-targeted antioxidant can inhibit peroxidase activity of cytochrome c by detachment of the protein from liposomes. *FEBS Lett.* **590,** 2836-2843

17. Aluri, H. S., Simpson, D. C., Allegood, J. C., Hu, Y., Szczepanek, K., Gronert, S., Chen, Q., and Lesnefsky, E. J. (2014) Electron flow into cytochrome c coupled with reactive oxygen species from the electron transport chain converts cytochrome c to a cardiolipin peroxidase: role during ischemia-reperfusion. *Biochim. Biophys. Acta.* **1840,** 3199-3207
18. Josephs, T. M., Morison, I. M., Day, C. L., Wilbanks, S. M., and Ledgerwood, E. C. (2014) Enhancing the peroxidase activity of cytochrome c by mutation of residue 41: implications for the peroxidase mechanism and cytochrome c release. *Biochem. J.* **458,** 259-265
19. Puchkov, M. N., Vassarais, R. A., Korepanova, E. A., and Osipov, A. N. (2013) Cytochrome c produces pores in cardiolipin-containing planar bilayer lipid membranes in the presence of hydrogen peroxide. *Biochim. Biophys. Acta.* **1828,** 208-212
20. Tyurina, Y. Y., Kini, V., Tyurin, V. A., Vlasova, I. I., Jiang, J., Kapralov, A. A., Belikova, N. A., Yalowich, J. C., Kurnikov, I. V., and Kagan, V. E. (2006) Mechanisms of cardiolipin oxidation by cytochrome c: relevance to pro- and antiapoptotic functions of etoposide. *Mol. Pharmacol.* **70,** 706-717
21. Harel, S., Salan, M. A., and Kanner, J. (1988) Iron release from metmyoglobin, methaemoglobin and cytochrome c by a system generating hydrogen peroxide. *Free Radic. Res. Commun.* **5,** 11-19
22. Yurkova, I., Huster, D., and Arnhold, J. (2009) Free radical fragmentation of cardiolipin by cytochrome c. *Chem. Phys. Lipids.* **158,** 16-21
23. Kim, N. H., Jeong, M. S., Choi, S. Y., and Kang, J. H. (2006) Oxidative modification of cytochrome c by hydrogen peroxide. *Mol. Cells.* **22,** 220-227
24. Radi, R., Turrens, J. F., and Freeman, B. A. (1991) Cytochrome c-catalyzed membrane lipid peroxidation by hydrogen peroxide. *Arch. Biochem. Biophys.* **288,** 118-125
25. Yin, V., Shaw, G. S., and Konermann, L. (2017) Cytochrome c as a peroxidase: activation of the precatalytic native state by H_2O_2-induced covalent modifications. *J. Am. Chem. Soc.* **139,** 15701-15709
26. Chen, Y. R., Chen, C. L., Chen, W., Zweier, J. L., Augusto, O., Radi, R., and Mason, R. P. (2004) Formation of protein tyrosine ortho-semiquinone radical and nitrotyrosine from cytochrome c-derived tyrosyl radical. *J. Biol. Chem.* **279,** 18054-18062
27. Annibal, A., Colombo, G., Milzani, A., Dalle-Donne, I., Fedorova, M., and Hoffmann, R. (2016) Identification of dityrosine cross-linked sites in oxidized human serum albumin. *J. Chromatogr. B Analyt. Technol. Biomed. Life Sci.* **1019,** 147-155
28. Klema, V. J. and Wilmot, C. M. (2012) The role of protein crystallography in defining the mechanisms of biogenesis and catalysis in copper amine oxidase. *Int. J. Mol. Sci.* **13,** 5375-5405
29. Ott, M., Robertson, J. D., Gogvadze, V., Zhivotovsky, B., and Orrenius, S. (2002) Cytochrome c release from mitochondria proceeds by a two-step process. *Proc. Natl. Acad. Sci. U. S. A.* **99,** 1259-1263
30. Alvarez-Paggi, D., Hannibal, L., Castro, M. A., Oviedo-Rouco, S., Demicheli, V., Tortora, V., Tomasina, F., Radi, R., and Murgida, D. H. (2017) Multifunctional cytochrome c: learning new tricks from an old dog. *Chem. Rev.* **117,** 13382-13460
31. Mohammadyani, D., Yanamala, N., Samhan-Arias, A. K., Kapralov, A. A., Stepanov, G., Nuar, N., Planas-Iglesias, J., Sanghera, N., Kagan, V. E., and Klein-Seetharaman, J. (2018) Structural characterization of cardiolipin-driven activation of cytochrome c into a peroxidase and membrane perturbation. *Biochim. Biophys. Acta.* **1860,** 1057-1068
32. Moreno-Beltran, B., Guerra-Castellano, A., Diaz-Quintana, A., Del, C. R., Garcia-Maurino, S. M., Diaz-Moreno, S., Gonzalez-Arzola, K., Santos-Ocana, C., Velazquez-Campoy, A., De la Rosa, M. A., Turano, P., and Diaz-Moreno, I. (2017) Structural basis of mitochondrial dysfunction in response to cytochrome c phosphorylation at tyrosine 48. *Proc. Natl. Acad. Sci. U. S. A* **114,** E3041-E3050
33. Fedorova, M. (2017) Diversity of protein carbonylation pathways: direct oxidation, glycoxidation and modifications by lipid peroxidation products. In Joaquim Ros, editor. *Protein Carbonylation: Principles, Analysis, and Biological Implications*, John Wiley & Sons, Inc.

34. Isom, A. L., Barnes, S., Wilson, L., Kirk, M., Coward, L., and Darley-Usmar, V. (2004) Modification of cytochrome c by 4-hydroxy- 2-nonenal: evidence for histidine, lysine, and arginine-aldehyde adducts. *J. Am. Soc. Mass Spectrom.* **15,** 1136-1147
35. Sinibaldi, F., Milazzo, L., Howes, B. D., Piro, M. C., Fiorucci, L., Polticelli, F., Ascenzi, P., Coletta, M., Smulevich, G., and Santucci, R. (2017) The key role played by charge in the interaction of cytochrome c with cardiolipin. *J. Biol. Inorg. Chem.* **22,** 19-29
36. Margoliash, E. and Frowirt, N. (1959) Spectrum of horse-heart cytochrome c. *Biochem. J.* **71,** 570-572
37. Beers, R. F., Jr. and Sizer, I. W. (1952) A spectrophotometric method for measuring the breakdown of hydrogen peroxide by catalase. *J. Biol. Chem.* **195,** 133-140
38. Noble, R. W. and Gibson, Q. H. (1970) The reaction of ferrous horseradish peroxidase with hydrogen peroxide. *J. Biol. Chem.* **245,** 2409-2413
39. Miyamoto, S., Nantes, I. L., Faria, P. A., Cunha, D., Ronsein, G. E., Medeiros, M. H., and Di, M. P. (2012) Cytochrome c-promoted cardiolipin oxidation generates singlet molecular oxygen. *Photochem. Photobiol. Sci.* **11,** 1536-1546
40. Barlett, G. R. (1959) Phosphorus assay in column chromatography. *J. Biol. Chem.* **234,** 466-468
41. Göse, M., Pescador, P., and Reibetanz, U. (2015) Design of a homogeneous multifunctional supported lipid membrane on layer-by-layer coated microcarriers. *Biomacromolecules.* **16,** 757-768
42. Nakamura, T. and Maeda, H. (1991) A simple assay for lipid hydroperoxides based on triphenylphosphine oxidation and high-performance liquid chromatography. *Lipids* **26,** 765-768
43. Re, R., Pellegrini, N., Proteggente, A., Pannala, A., Yang, M., and Rice-Evans, C. (1999) Antioxidant activity applying an improved ABTS radical cation decolorization assay. *Free Radic. Biol. Med.* **26,** 1231-1237
44. Zschaler, J., Dorow, J., Schope, L., Ceglarek, U., and Arnhold, J. (2015) Impact of myeloperoxidase-derived oxidants on the product profile of human 5-lipoxygenase. *Free Radic. Biol. Med.* **85,** 148-156
45. Stookey, L. L. (1970) Ferrozine - a new spectrophotometric reagent for iron. *Anal. Chem.* **42,** 779-781
46. Mandal, B., Sinha, P. K., Sen, R., and Mandal, A. K. (2016) A comparative spectrophotometric study using ferrozine and 1,10-ortho-phenanthroline to evaluate the iron redox ratio (Fe(2+)/sigmaFe) in glass prepared by microwave heating. *Anal. Sci.* **32,** 571-576
47. Maitra, D., Byun, J., Andreana, P. R., Abdulhamid, I., Saed, G. M., Diamond, M. P., Pennathur, S., and Abu-Soud, H. M. (2011) Mechanism of hypochlorous acid-mediated heme destruction and free iron release. *Free Radic. Biol. Med.* **51,** 364-373
48. Griesser, E., Vemula, V., Raulien, N., Wagner, U., Reeg, S., Grune, T., and Fedorova, M. (2017) Cross-talk between lipid and protein carbonylation in a dynamic cardiomyocyte model of mild nitroxidative stress. *Redox. Biol.* **11,** 438-455
49. Bradford, M. M. (1976) A rapid and sensitive method for the quantitation of microgram quantities of protein utilizing the principle of protein-dye binding. *Anal. Biochem.* **72,** 248-254
50. Vemula, V., Ni, Z., and Fedorova, M. (2015) Fluorescence labeling of carbonylated lipids and proteins in cells using coumarin-hydrazide. *Redox. Biol.* **5,** 195-204
51. Schneider, C. A., Rasband, W. S., and Eliceiri, K. W. (2012) NIH Image to ImageJ: 25 years of image analysis. *Nat. Methods* **9,** 671-675
52. Belikova, N. A., Vladimirov, Y. A., Osipov, A. N., Kapralov, A. A., Tyurin, V. A., Potapovich, M. V., Basova, L. V., Peterson, J., Kurnikov, I. V., and Kagan, V. E. (2006) Peroxidase activity and structural transitions of cytochrome c bound to cardiolipin-containing membranes. *Biochemistry* **45,** 4998-5009

Table 1. Summary of cyt c modifications identified by gel-based bottom-up LC-MS/MS experiments in the absence, or presence of H_2O_2, TLCL or combination of both. Cyt c (100 μM) was incubated in ammonium bicarbonate buffer alone, in the presence of H_2O_2 (1mM), TLCL (10 mM) or combination of both for 30- and 60-min. Proteins were separate by SDS-PAGE, digested with trypsin and analyzed by LC-MS/MS. PTMs were identified from obtained tandem mass spectra using search engine assisted database search.

Sample	H_2O_2	TLCL	Time	Cyt c sequence with marked modifications Red – oxidative PTMs, yellow – adducts with glyoxal and acrolein; blue – adducts with HNE and ONE; green – diTyr crosslinks									
1			0’	MGDVEKGKKI	FVQKCAQCHT	VEKGGKHKTG	PNLHGLFGRK	TGQAPGFSYT	DANKNKGITW	GEETLMEYLE	NPKKYIPGTK	MIFAGIKKKG	EREDLIAYLK	KATNE
2			30’	MGDVEKGKKI	FVQKCAQCHT	VEKGGKHKTG	PNLHGLFGRK	TGQAPGFSYT	DANKNKGITW	GEETLMEYLE	NPKKYIPGTK	MIFAGIKKKG	EREDLIAYLK	KATNE
3			60’	MGDVEKGKKI	FVQKCAQCHT	VEKGGKHKTG	PNLHGLFGRK	TGQAPGFSYT	DANKNKGITW	GEETLMEYLE	NPKKYIPGTK	MIFAGIKKKG	EREDLIAYLK	KATNE
4	+		30’	MGDVEKGKKI	FVQKCAQCHT	VEKGGKHKTG	PNLHGLFGRK	TGQAPGFSYT	DANKNKGITW	GEETLMEYLE	NPKKYIPGTK	MIFAGIKKKG	EREDLIAYLK	KATNE
5	+		60’	MGDVEKGKKI	FVQKCAQCHT	VEKGGKHKTG	PNLHGLFGRK	TGQAPGFSYT	DANKNKGITW	GEETLMEYLE	NPKKYIPGTK	MIFAGIKKKG	EREDLIAYLK	KATNE
6		+	0’	MGDVEKGKKI	FVQKCAQCHT	VEKGGKHKTG	PNLHGLFGRK	TGQAPGFSYT	DANKNKGITW	GEETLMEYLE	NPKKYIPGTK	MIFAGIKKKG	EREDLIAYLK	KATNE
7		+	30’	MGDVEKGKKI	FVQKCAQCHT	VEKGGKHKTG	PNLHGLFGRK	TGQAPGFSYT	DANKNKGITW	GEETLMEYLE	NPKKYIPGTK	MIFAGIKKKG	EREDLIAYLK	KATNE
8		+	60’	MGDVEKGKKI	FVQKCAQCHT	VEKGGKHKTG	PNLHGLFGRK	TGQAPGFSYT	DANKNKGITW	GEETLMEYLE	NPKKYIPGTK	MIFAGIKKKG	EREDLIAYLK	KATNE
9	+	+	30’	MGDVEKGKKI	FVQKCAQCHT	VEKGGKHKTG	PNLHGLFGRK	TGQAPGFSYT	DANKNKGITW	GEETLMEYLE	NPKKYIPGTK	MIFAGIKKKG	EREDLIAYLK	KATNE
10	+	+	60’	MGDVEKGKKI	FVQKCAQCHT	VEKGGKHKTG	PNLHGLFGRK	TGQAPGFSYT	DANKNKGITW	GEETLMEYLE	NPKKYIPGTK	MIFAGIKKKG	EREDLIAYLK	KATNE
					10	20	30	40	50	60	70	80	90	100

Table 2. Binding constants for cyt c incubated in the absence and presence of H_2O_2 with TLCL-containing liposomes. POPC (negative control) and POPC/TLCL liposomes (1 mM of total lipid) were incubated with cyt c (20 μM; incubated in the absence or presence of H_2O_2 (1 mM) for 0, 30, and 60 min), NAO was added after 30 min for another 1 h. Samples were separated by native PAGE in reverse mode and fluorescence of unbound NAO was measured using signal from POPC liposome (no binding) as negative control.

			***K* binding constant (K_a) ± SEM, x 10^7 M^{-1}[‡]**	
	H_2O_2	**Time (min)**	**TLCL-Liposomes**	**P-value[§]**
Unoxidized cyt c	-	0	15.4 ± 1.08	-
	-	30	14.8 ± 2.46	ns (0.8864)
	-	60	15.0 ± 0.70	ns (0.8281)
Oxidized cyt c	+	0	13.1 ± 1.54	ns (0.3728)
	+	30	5.02 ± 1.98	* (0.0199)
	+	60	4.29 ± 2.55	* (0.0309)

[‡]Data are expressed as mean ± SEM (n=3). SEM: the standard error of the mean. [§]Comparisons between the control group (unoxidized cyt c at 0 min) and each other groups were performed using the t-test. *Significant differences with $P < 0.05$ vs. control group.

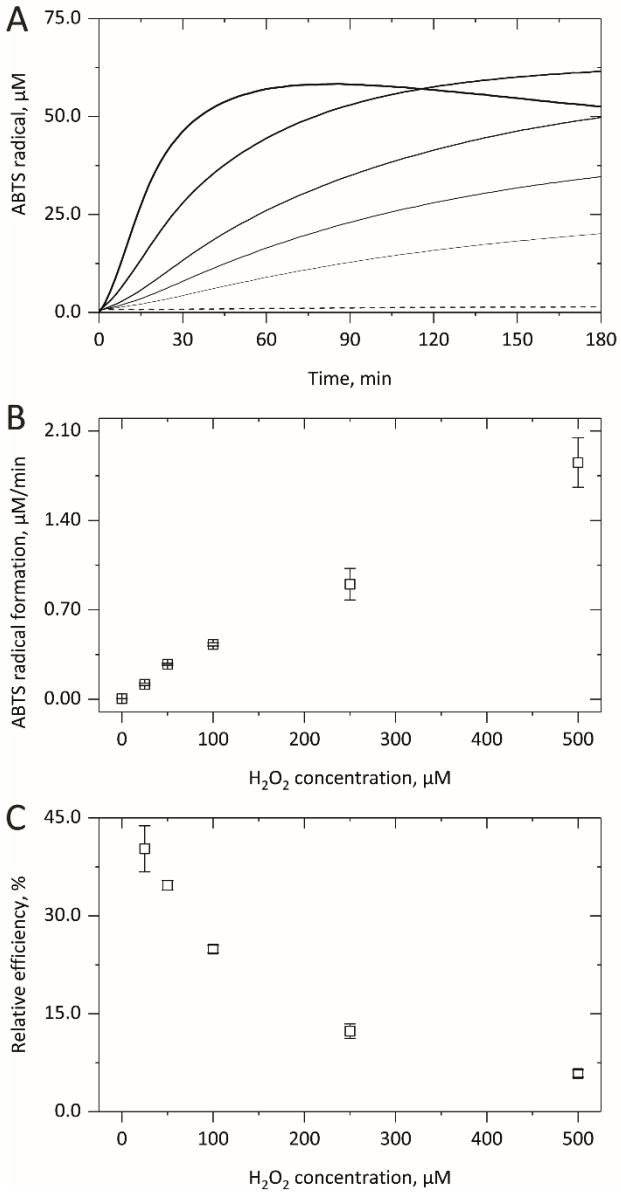

Figure 1. H_2O_2-dependent peroxidase activity of cytochrome c. After adding up to 500 µM H_2O_2 to 5 µM cyt c the formation of $ABTS^{+\bullet}$ from 1 mM ABTS in 10 mM PP (pH 7.4) was followed for up to 3 h at 37 °C by monitoring the absorbance increase at 734 nm. The kinetic curves in (A) illustrate that in the presence of increasing H_2O_2 concentrations (straight lines: 25, 50, 100, 250 and 500 µM) a shorter lag phase, a higher linear $ABTS^{+\bullet}$ formation rate and a quicker deactivation of the cyt c-based peroxidase activity were observed. In (B) the linear increase of the cyt-c-derived enzymatic activity with the H_2O_2 concentration is shown, in (C) the coinciding exponential decrease in the relative efficiency of the cyt c-derived peroxidase activity is illustrated. While in (A) averaged kinetic curves from 3 independent experiments are shown in (B) and (C) the corresponding mean and SD values are given.

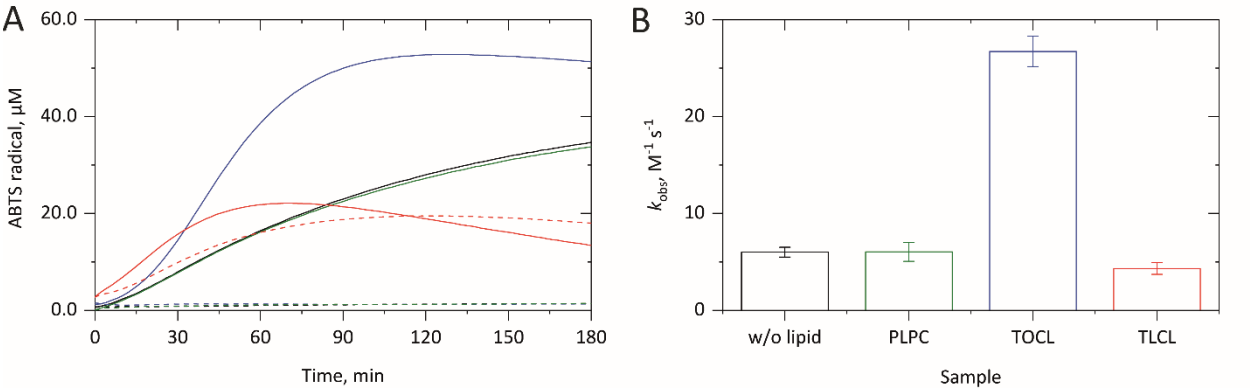

Figure 2. Effect of cardiolipin on cytochrome c peroxidase activity. After pre-incubating 5 µM cyt c in 10 mM PP(pH 7.4) with liposomes (500 µM lipid concentration) in 10 mM PP (pH 7.4) 50 µM H_2O_2 was added and the formation of $ABTS^{+\bullet}$ from 1 mM ABTS was followed for up to 3 h at 37 °C by monitoring the absorbance increase at 734 nm. The kinetic curves in (A) show that PLPC (green) has no effect on the cyt c-based peroxidase activity, either in the presence (straight line) or in the absence (dashed line) of H_2O_2. TOCL (blue) strongly promotes the H_2O_2-derived cyt c-based peroxidase activity. TLCL (red) also supports the H_2O_2-derived cyt c peroxidase activity promotion but also activates this enzymatic activity on its own. In (B) the H_2O_2-derived increase in the peroxidase-activity of cyt c is shown for the lipid-free system (black) as well as for liposomes with the named lipids. In (A) averaged kinetic curves from 3 independent experiments are shown while in (B) the corresponding mean and SD values are given. Effect of cardiolipins on cyt c peroxidase activity. $ABTS^{+\bullet}$ production (A) and peroxidase activity (B) of cyt c (5 µM) was measured in the presence of liposomes (500 µM lipid concentration) containing PLPC (green), TOCL (blue) or TLCL (red) without (dashed) or with (straight) H_2O_2 (50 µM) for 180 min. Averaged kinetic curves (A) and the corresponding mean and SD values (B) from 3 independent measurements are shown.

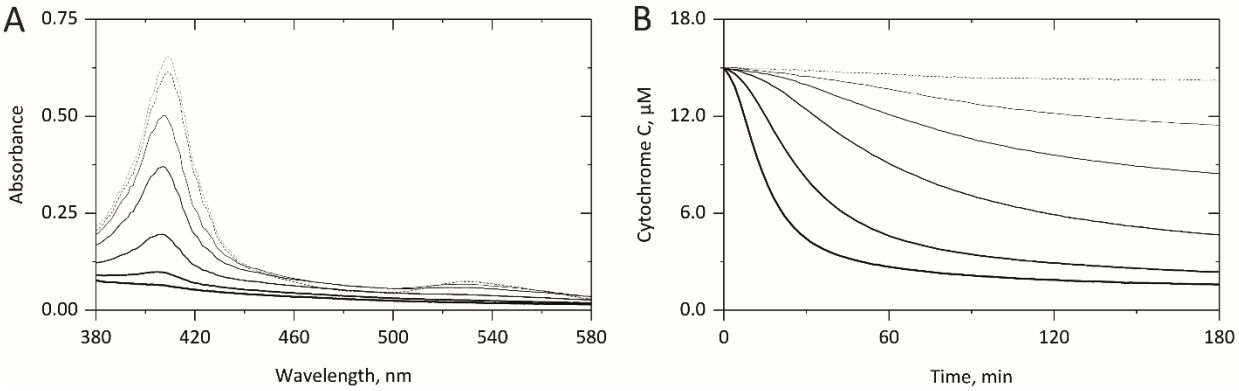

Figure 3. H_2O_2-derived degradation of cytochrome c. 15 µM cyt c were incubated in 10 mM PP (pH 7.4) either in the absence (dashed) or presence of H_2O_2 (straight lines: 75, 150, 300, 750, 1500 µM) for 3 h at 37 °C. As shown in (A) while in the absence of H_2O_2 an incubation time of 3 h did not result in significant spectral changes (compare grey and black dashed lines) the incubation with H_2O_2 for 3 h led to a concentration-dependent decrease in the Soret band and also the heme-derived bands beyond 510 nm. As shown in (B) by continuously monitoring the loss of the Soret band a H_2O_2-concentration-dependent loss of the Soret band was observed, indicating a progressive loss of heme-containing cyt c. Averaged curves from 3 independent experiments are given.

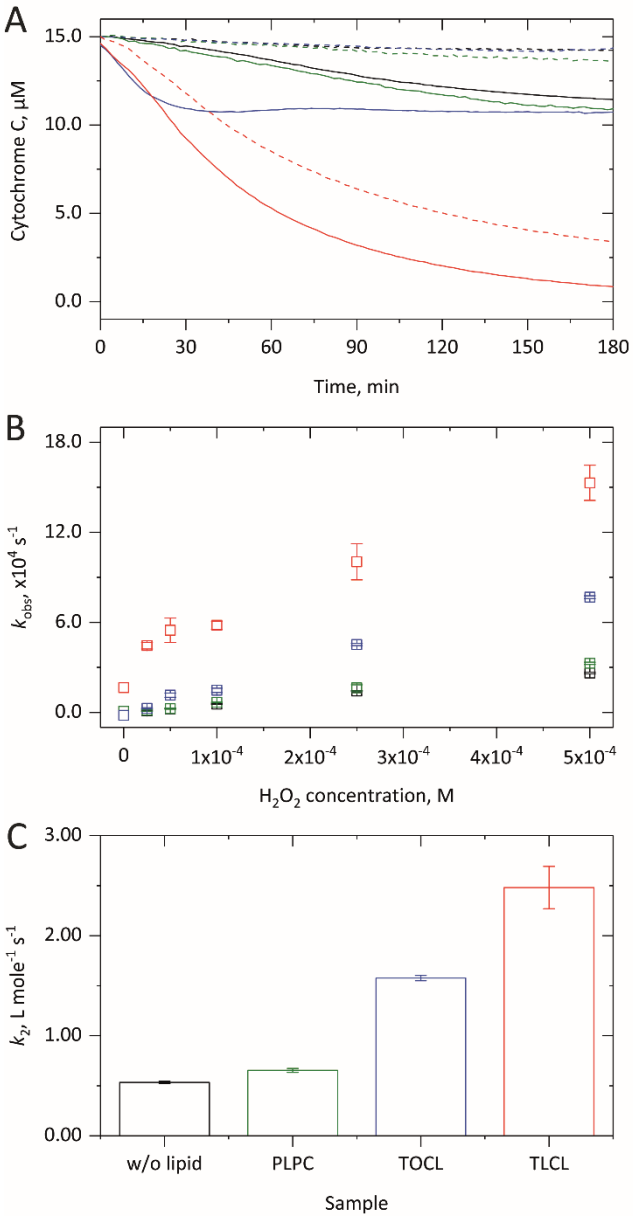

Figure 4. Effect of cardiolipin on the degradation of cytochrome c.15 µM cyt c were incubated in the absence or presence of 1.5 mM liposomes with up to 500 µM H_2O_2 in 10 mM PP (pH 7.4) at 37 °C for up to 3 h. As shown in (A) both in the absence of lipid (black) and in the presence of PLPC (green) in the absence of H_2O_2 (dashed) no heme degradation occurs while in its presence (75 µM, straight) a small heme loss takes place. With TOCL (blue) in the presence of H_2O_2 comparable heme degradation is observed with a faster kinetics. After pre-incubation with TLCL (red) even in the absence of H_2O_2 a quick and more substantial heme degradation takes place which, in the additional presence of H_2O_2, leads to a complete heme loss. In (B) the k_{obs} value obtained from the linear phase of the Soret band decrease is replotted against the H_2O_2 concentration and always exhibit a linear relationship. As shown in (C) from the corresponding slopes k_2 values for the H_2O_2-derived heme degradation were calculated, showing considerably higher values in the presence of CL-containing liposomes. In (A) averaged kinetic curves from 3 independent measurements are shown, in (B) and (C) the corresponding mean and SD values are shown.

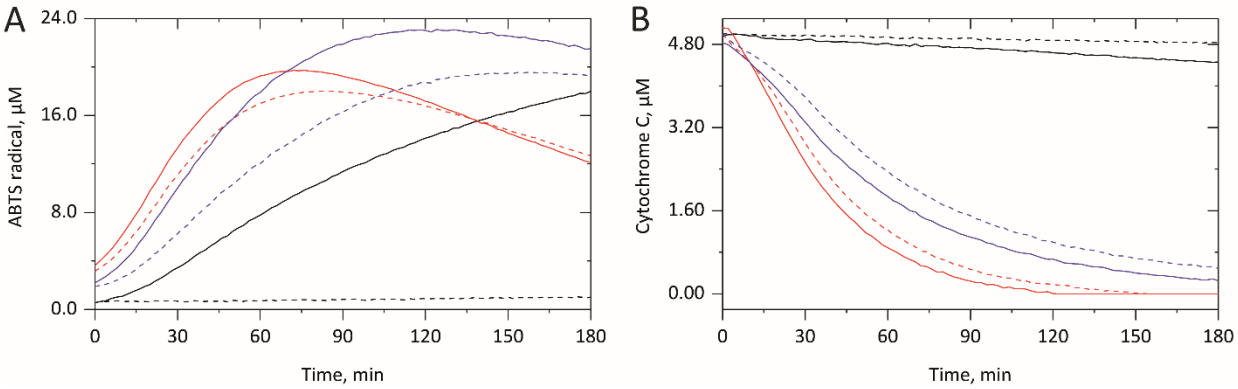

Figure 5. Role of cardiolipin-derived lipid hydroperoxides reduction on cyt c peroxidase activity and enzyme degradation. In (A) peroxidase activity measurements were performed in the absence (black) of lipid or in the presence of liposomes (500 µM lipid concentration) containing non-reduced (red) or reduced (violet) TLCL by incubating 5 µM cyt c without (dashed) or with (straight) 25 µM H_2O_2 for 180 min in 10 mM PP at 37 °C. ABTS radical formation from 1 mM ABTS was monitored at 734 nm. The strong peroxidase activity-promoting effects of TLCL both in the absence and presence of H_2O_2 are considerably inhibited by previous reduction of the LOOH amount. As shown in (B) also the H_2O_2-independent TLCL-derived heme degradation in cyt c is considerably disturbed by reducing the LOOH amount. Averaged kinetic curves from 3 independent experiments are displayed.

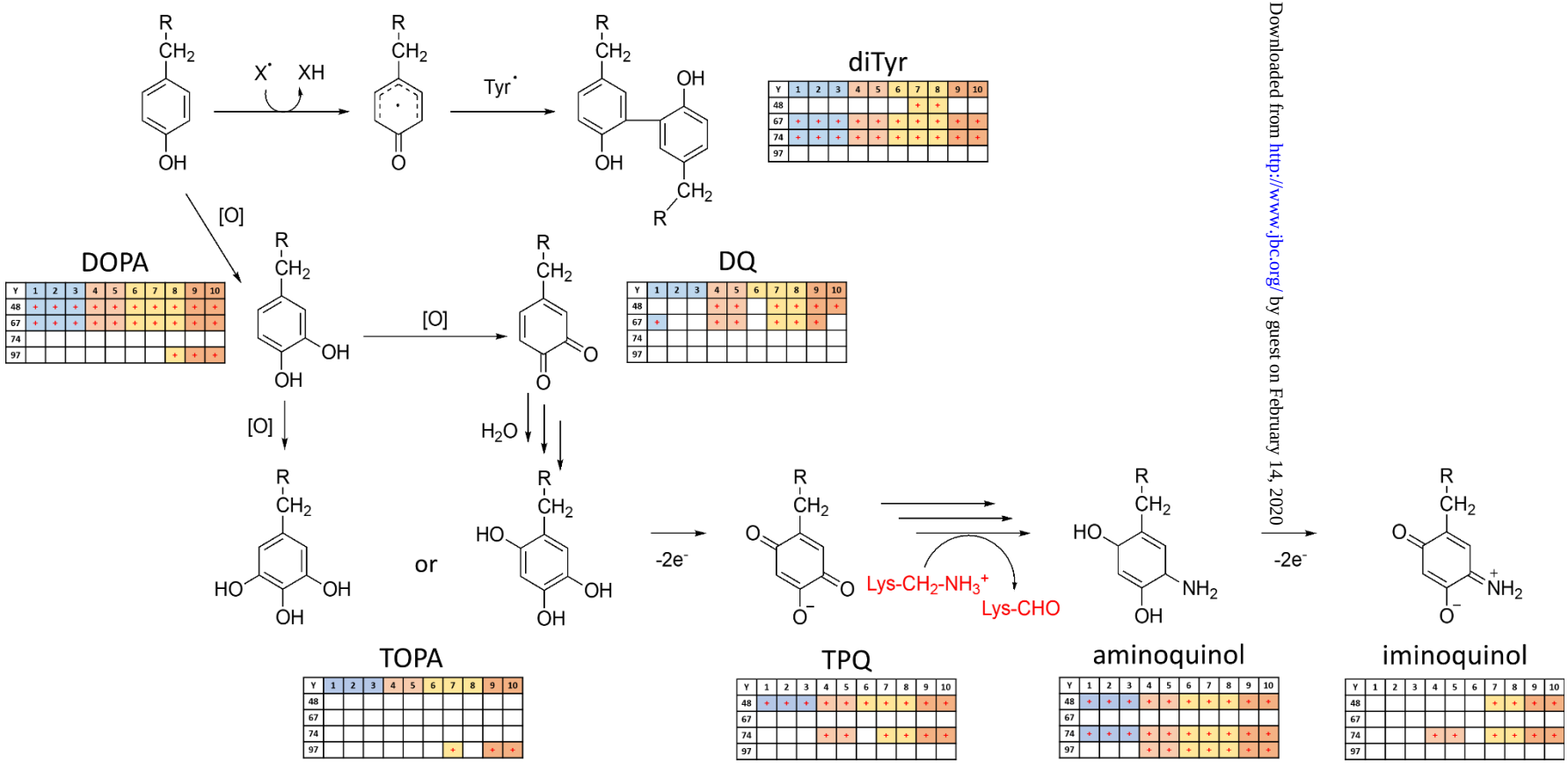

Figure 6. Proposed pathway of Tyr residues oxidation in cyt c protein leading to the auto-generation of trihydroxyphenylalanine quinone (TPQ) followed by Lys residue deamination to aminoadipic semialdehyde. Inserts demonstrate results of MS/MS based identification of corresponding modifications on Tyr 48, 67, 74, and 97 residues of cyt c in the absence (columns 1-3, blue), or presence of H_2O_2 (columns 4-5, red), TLCL (columns 6-8, yellow) or combination of both (columns 9-10, orange)**.** diTyr - dityrosine cross-links, DOPA - dihydroxyphenylalanine, DQ – dihydroxyphenylalanine quinone, TOPA - trihydroxyphenylalanine, TPQ - trihydroxyphenylalanine quinone.

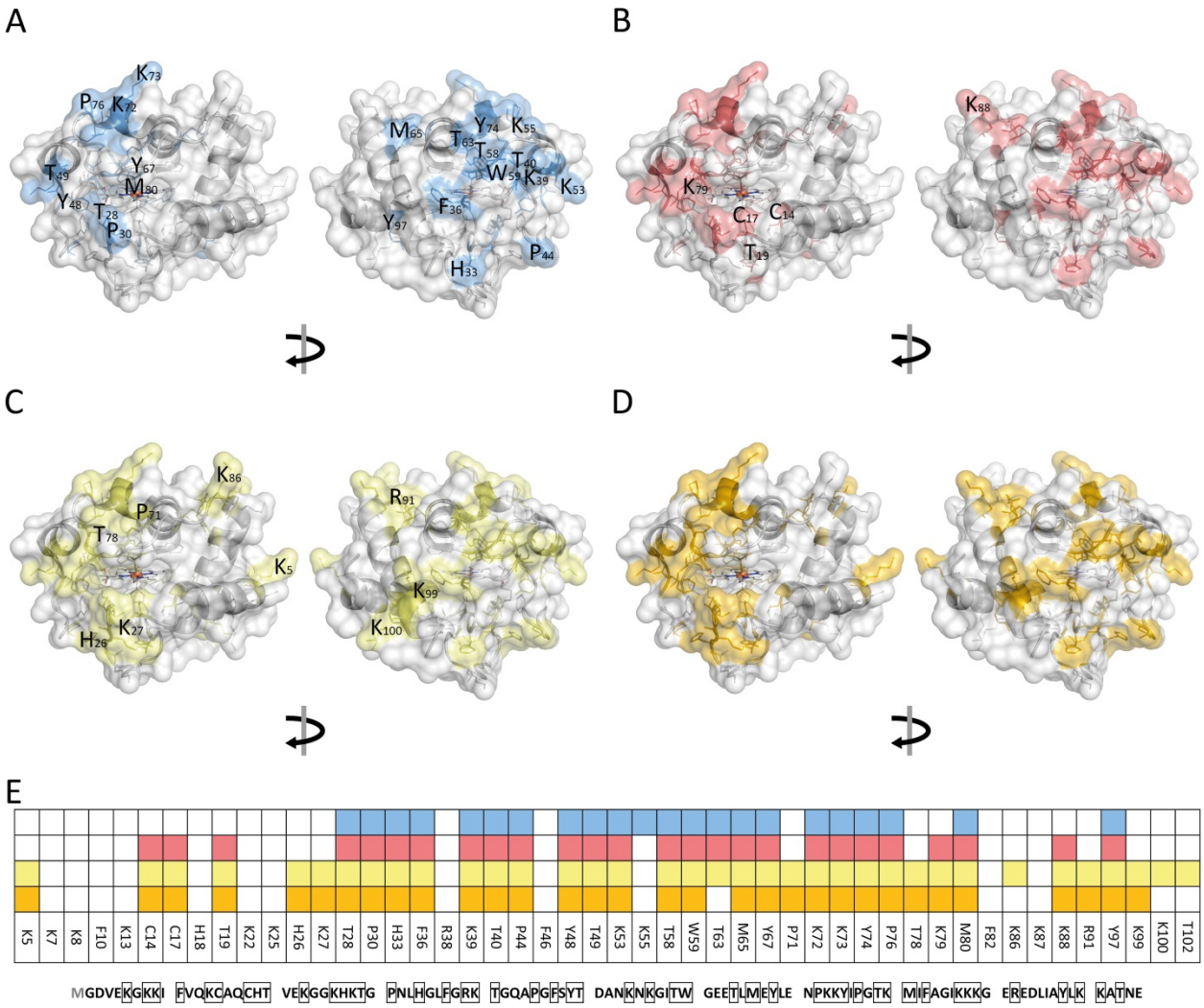

Figure 7. Modification of cytochrome c identified by LC-MS/MS in control (A), H_2O_2 (B), TLCL (C), H_2O_2, TLCL (D) incubations and a summary of all (E). Cyt c (100 μM) was incubated in ammonium bicarbonate buffer alone, in the presence of H_2O_2 (1 mM), TLCL (10 mM) or combination of both for 30 and 60 min. Proteins were separate by SDS-PAGE, digested with trypsin and analyzed by LC-MS/MS. PTMs were identified from obtained tandem mass spectra using search engine assisted database search. Tertiary structure elements of the protein are shown in cartoon representation while the surface is shown semitransparent. Amino acid residues representing possible PTM sites are shown as sticks whereby the residues on which modifications were detected are shown in blue (autoxidation), red (oxidation after incubation with H_2O_2), green (TLCL), and orange (H_2O_2 and TLCL). For panel B, C, and D only new modifications sites, not present in untreated samples are marked with amino acid one letter code and position. The model based on the pdb entry 2b4z (cyt c from bovine heart, 1.5 Å resolution) was used and modified with pymol v.0.99.

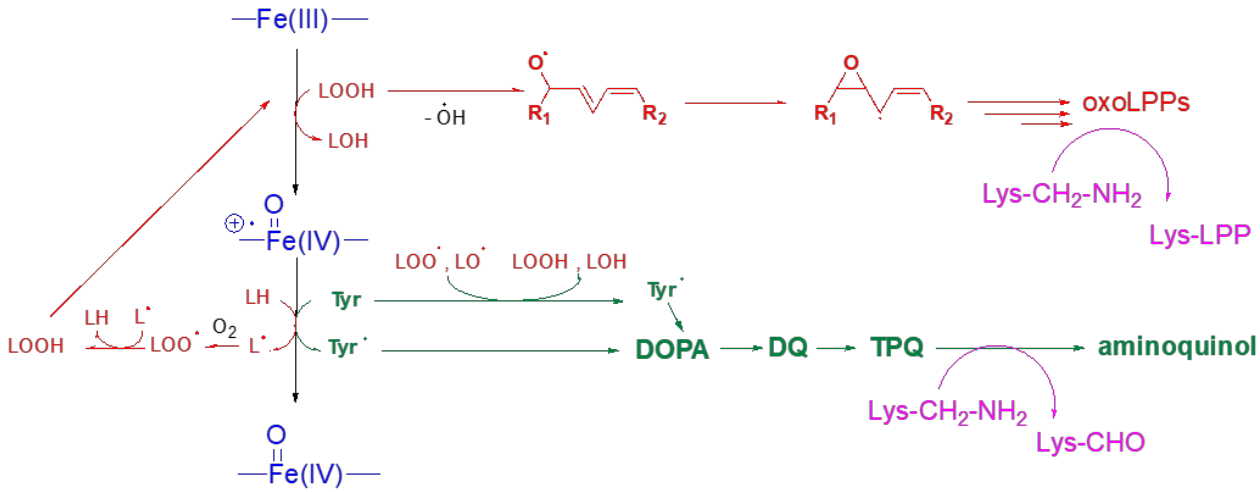

Figure 8. Summary of proposed reaction mechanisms leading to TLCL (red route) and protein (green) oxidative modifications including Lys deamination to aminoadipic semialdehyde or adducts formation with carbonylated LPPs (purple) during cyt c peroxidase cycle (blue). LOOH represents CL-derived lipid peroxide. DOPA - dihydroxyphenylalanine, DQ – dihydroxyphenylalanine quinone, oxoLPPs – carbonylated lipid peroxidation products, TPQ - trihydroxyphenylalanine quinone.

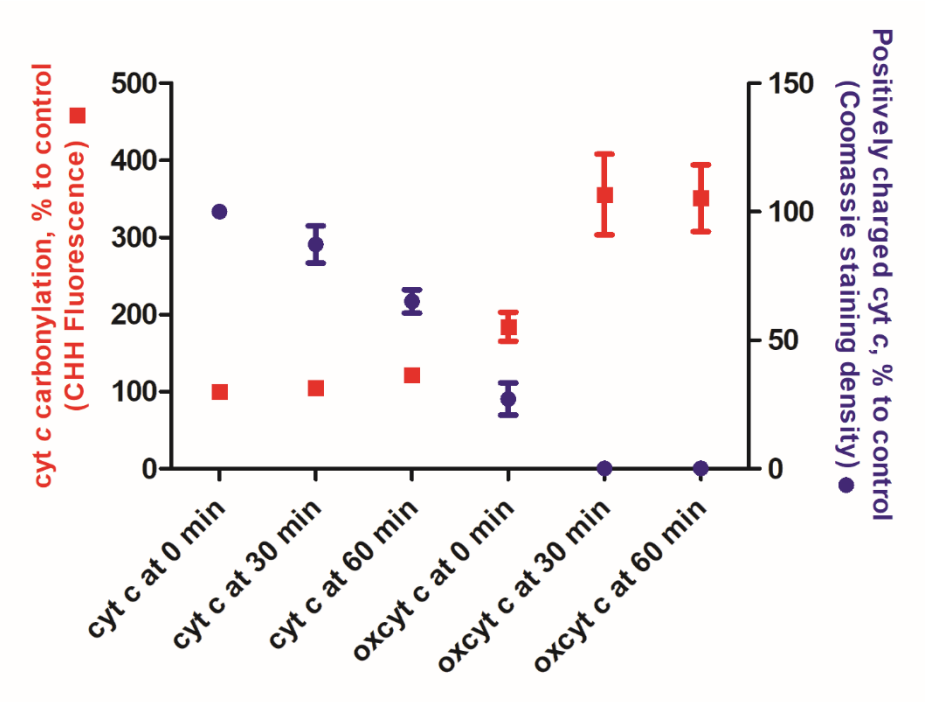

Figure 9. Cyt c carbonylation and associated loss of positive charge upon oxidation with hydrogen peroxide. Cyt c (100 μM) was incubated in the absence or presence of H_2O_2 (1 mM) for 0, 30, and 60 min. Protein carbonylation (left axis, red) was quantified relative to control (cyt c incubated in the absence of hydrogen peroxide for 0 min) using derivatization with carbonyl specific fluorescence dye CHH and SDS-PAGE separation. Reduction of cyt c positive charge (right axis, blue) was quantified relative to control (cyt c incubated in the absence of hydrogen peroxide for 0 min) using native PAGE performed in reverse electrophoresis mode. Data are expressed as mean ± SEM (n=3).

Cytochrome c auto-catalyzed carbonylation in the presence of hydrogen peroxide and cardiolipins

Uladzimir Barayeu, Mike Lange, Lucía Méndez, Jürgen Arnhold, Oleg I. Shadyro, Maria Fedorova and Jörg Flemmig

J. Biol. Chem. published online December 12, 2018
